10-1-2004

Stability Analysis of Legged Locomotion Models by Symmetry-Factored Return Maps

Richard Altendorfer
University of Michigan

Daniel E. Koditschek
University of Pennsylvania, kod@seas.upenn.edu

Philip Holmes
Princeton University

Reprinted from *The International Journal of Robotics Research*, Volume 23, Issue 10-11, October-November 2004, pages 979-999.
DOI: 10.1177/0278364904047389

Stability Analysis of Legged Locomotion Models by Symmetry-Factored Return Maps

Abstract
We present a new stability analysis for hybrid legged locomotion systems based on the "symmetric" factorization of return maps.We apply this analysis to two-degrees-of-freedom (2DoF) and threedegrees- of-freedom (3DoF) models of the spring loaded inverted pendulum (SLIP) with different leg recirculation strategies. Despite the non-integrability of the SLIP dynamics, we obtain a necessary condition for asymptotic stability (and a sufficient condition for instability) at a fixed point, formulated as an exact algebraic expression in the physical parameters. We use this expression to characterize analytically the sensory cost and stabilizing benefit of various feedback schemes previously proposed for the 2DoF SLIP model, posited as a low-dimensional representation of running.We apply the result as well to a 3DoF SLIP model that will be treated at greater length in a companion paper as a descriptive model for the robot RHex.

Keywords
legged locomotion, hybrid system, return map, spring loaded inverted pendulum, stability, time-reversal, symmetry

Comments
Reprinted from *The International Journal of Robotics Research*, Volume 23, Issue 10-11, October-November 2004, pages 979-999.
DOI: 10.1177/0278364904047389

Stability Analysis of Legged Locomotion Models by Symmetry-Factored Return Maps

Richard Altendorfer, Daniel E. Koditschek and Philip Holmes

The International Journal of Robotics Research 2004; 23; 979
DOI: 10.1177/0278364904047389

Richard Altendorfer
Daniel E. Koditschek

Department of Electrical Engineering and Computer Science
University of Michigan
Ann Arbor, MI 48109, USA

Philip Holmes

Department of Mechanical and Aerospace Engineering
Princeton University
Princeton, NJ 08544, USA

Stability Analysis of Legged Locomotion Models by Symmetry-Factored Return Maps

Abstract

We present a new stability analysis for hybrid legged locomotion systems based on the "symmetric" factorization of return maps. We apply this analysis to two-degrees-of-freedom (2DoF) and three-degrees-of-freedom (3DoF) models of the spring loaded inverted pendulum (SLIP) with different leg recirculation strategies. Despite the non-integrability of the SLIP dynamics, we obtain a necessary condition for asymptotic stability (and a sufficient condition for instability) at a fixed point, formulated as an exact algebraic expression in the physical parameters. We use this expression to characterize analytically the sensory cost and stabilizing benefit of various feedback schemes previously proposed for the 2DoF SLIP model, posited as a low-dimensional representation of running. We apply the result as well to a 3DoF SLIP model that will be treated at greater length in a companion paper as a descriptive model for the robot RHex.

KEY WORDS—legged locomotion, hybrid system, return map, spring loaded inverted pendulum, stability, time-reversal symmetry

1. Introduction

In this paper we introduce a new formalism for studying the stability of dynamical legged locomotion gaits and other periodic dynamically dextrous robotic tasks. We are motivated in part by the need to explain and control the remarkable performance of RHex, an autonomous hexapedal running machine whose introduction has broken all prior published records for speed, specific resistance, and mobility over broken terrain (Saranli, Buehler, and Koditschek 2001). When RHex is properly tuned it exhibits sagittal plane center of mass (COM) trajectories well modeled by the spring loaded inverted pendulum (SLIP; Altendorfer et al. 2001), depicted in Figure 1. Indeed, this reflects the machine's bio-inspired origins, since animal (Blickhan and Full 1993) and human (Schwind 1998) runners exhibit sagittal plane COM trajectories similarly well described by the SLIP model. Moreover, the introduction by Raibert (1986) of the first dynamically stable running robots embodied the literal SLIP morphology. Thus, while other interesting hybrid Hamiltonian models of robotics are likely to be amenable, we focus the development of our new analytical method on variations of the SLIP running model.

1.1. SLIP Model as a Template for RHex

A general framework for "anchoring templates" like the SLIP mechanics in the far more elaborate morphologies of the bodies of real animals has been introduced in Full and Koditschek (1999). Briefly, given a high-dimensional dynamical system—the "anchor"—which is believed to be a reasonably accurate model of an animal or robot, a "template" is a low-dimensional dynamical system whose steady state encodes the task and is conjugate to the restriction dynamics of the anchor on an attracting invariant submanifold. Much of the robotics work of Koditschek and colleagues relies upon this sort of construction (Buehler, Koditschek, and Kindlman 1990; Rizzi, Whitcomb, and Koditschek 1992; Nakanishi, Fukuda, and Koditschek 2000; Westervelt, Grizzle, and Koditschek 2003).

In general, both the anchoring as well as the control of the SLIP template seem to demand sensing, actuation, and computation that may be unrealistic relative to the resources that animals and practical robots might possess. Indeed, a hierarchical controller (Saranli 2002) for a RHex-like simulation model programmed in SimSect (Saranli 2000) that enforces both the anchoring as well as the template control relies on sophisticated full-state feedback. Only a portion of the sensor

The International Journal of Robotics Research
Vol. 23, No. 10–11, October–November 2004, pp. 979-999,
DOI: 10.1177/0278364904047389

suite necessary to implement this feedback control has yet (only recently) been installed on the robot (Lin, Komsuoğlu, and Koditschek 2003) and it is currently unknown whether the stabilizing effect of this controller seen in simulation will persist in the presence of unavoidable sensor noise and unmodeled aspects of the mechanics. This motivates the question: is it possible to implement the template-anchor paradigm (Full and Koditschek 1999) with sensor-cheap, low-bandwidth controllers?

In this paper we address that part of the above question concerned with template control. Namely, given that a SLIP-anchoring mechanism is present, either by deliberate design or by the interaction of the controlled robot with its environment, can the stability and performance of the controlled template be assessed methodically (beyond empirical or numerical study), for example, as a function of the cost of the sensory feedback required?

1.2. Output Feedback Stabilization in the SLIP Model

The SLIP model is a hybrid dynamical system formed by the composition of leg–body stance dynamics with ballistic body flight dynamics. Control takes place during the flight phase, where the leg angle is set for the next touchdown event. The two-degrees-of-freedom (2DoF) SLIP model provides a ubiquitous description of biological runners in the sagittal plane (Blickhan and Full 1993) and also, as mentioned above, a broadly useful prescription for legged robot runners such as RHex (Raibert 1986; Saranli, Buehler, and Koditschek 2001; Altendorfer et al. 2001). The closely related 3DoF lateral leg spring (LLS) model has been recently identified as a candidate template for a cockroach running in the horizontal plane (Kubow and Full 1999; Schmitt and Holmes 2000) and seems likely to be relevant for RHex as well (Saranli, Buehler, and Koditschek 2001).

However, the limitations of the 2DoF SLIP model (no pitching dynamics, no lateral dynamics) and the 3DoF LLS model (failure to reproduce some aspects of animal data; Schmitt et al. 2002) show that far more sophisticated models will be required to capture more salient features of the anchor. In particular, a literal template of RHex, i.e., a model conjugate to the restriction dynamics of an attracting invariant submanifold in RHex, must include a source of dissipation as well as hip torques. Despite these shortcomings, the 2DoF SLIP and its extension to 3DoF (introduction of pitch dynamics) are sufficiently well motivated by prior literature, sufficiently mathematically challenging (due to their non-integrable nature) and their analysis sufficiently revealing of RHex-like properties (see the companion paper Altendorfer, Koditschek, and Holmes 2004) as to motivate our exclusive focus on them in this paper.

The stability properties of these hybrid dynamical systems can be assessed by a Poincaré or return map R acting on a (reduced) Poincaré section $\mathcal{X}$:

$$R : \mathcal{X} \to \mathcal{X} . \tag{1}$$

In legged locomotion, the iterates of this return map R—the function relating the body state at a periodically (at each stride) occurring event—summarizes all properties relevant to the goal of translating the body COM. The return map arises in general from a controlled plant model

$$\begin{aligned} x(k+1) &= A(x(k), u(k)) \\ y(k) &= C(x(k)) \end{aligned} \tag{2}$$

where the discrete time control input variable, $u(k)$, represents the consequences at the integrated stride-by-stride level of controlled influences imposed over continuous time within stance or flight. In this paper, physically motivated assumptions (listed in Section 2.4.1) that we impose upon the allowable continuous time influences turn out to yield a discrete time representative, u, that implicitly determines the flight time for the ballistic phase of the body at each stride. When the continuous time physical influences imposed within a given stride are determined according to state information gathered from the available observations of the previous stride, we have effectively introduced a discrete time feedback policy

$$u(k) = H(y(k)) \tag{3}$$

whose closed loop yields eq. (1), $R(x) = A(x, H \circ C(x))$. The controlled plant model for SLIP systems is specified in Section 2.4.3.

In this paper we confine our study exclusively to such time-invariant output feedback laws, H (eq. (3)) for two allied reasons. First, this restriction focuses attention on the key role played by the output function, C (eq. (2)), variations of which we will use to model sensor limitations of the underlying physical system represented by the SLIP model. Secondly, as u models the influence of flight phase duration (implicitly by specifying the leg angle trajectory), this restriction to time-invariant output feedback, H (eq. (3)), models the leg recirculation policies that have so rightly captured the attention of the legged locomotion community in recent years.

The surprising discovery of "self-stable" legged locomotion—first in the closely related LLS model (Schmitt and Holmes 2000), and subsequently in the SLIP itself (Seyfarth et al. 2002; Ghigliazza et al. 2003)—demands a more systematic account of what is meant by the term "self". In these studies, the duration of flight phase is determined by a fixed leg angle policy, and "self" connotes the apparent absence of active sensors. Recently, a more elaborate state-dependent leg retraction policy has been shown numerically to inherit the stability properties of the fixed touchdown angle policy while increasing the basin of the stable gait (Seyfarth, Geyer, and Herr 2003). On the other hand, a recirculation policy that initiates after leg liftoff a constant angular velocity until leg touchdown can induce neutral stability (Altendorfer, Koditschek,

and Holmes 2003). These apparently slightly varied policies mask significant variation in cost and effort depending upon how the sensor suite might be implemented in practice. We seek to shed greater light on when a more or less clever leg recirculation strategy can make a difference in the quality of gait stability (e.g., faster transients, larger basin) as a function of the "cost" of sensory data.

Of course, real sensors are not implemented in these templates at all but in physical machines. Empirically, it is abundantly clear that the leg swing policy plays a central role in the gait quality of physically useful machines such as RHex (Saranli, Buehler, and Koditschek 2001; Weingarten et al. 2004). Leg recirculation strategies have been shown numerically to play a key role in the gait quality of independent locomotion models inspired by quadrupedal animal trotters (Herr and McMahon 2000) and gallopers (Herr and McMahon 2001).

When the SLIP template is anchored actively (Saranli 2002) then its stability properties determine those of the anchor by definition; hence, insight into how to tune the quality of SLIP gaits transfers directly over to the physical machine of interest. The implications for gait quality of the physical machine in consequence of adjustments to leg recirculation derived from a passively anchored SLIP template are explored in the companion paper (Altendorfer, Koditschek, and Holmes 2004).

1.3. Contribution of this paper

Notwithstanding its apparent simplicity, the SLIP model is non-integrable: the stance phase trajectory cannot be written down in closed form—see, for example, Whittaker (1964) and Holmes (1990) for a discussion of the closely related restricted, planar, circular three-body problem—presenting us on first inspection with a control problem for which no exact "plant" model is available (Schwind and Koditschek 2000). This has motivated authors who seek insight more systematic than numerical simulation can provide to develop various physically motivated closed-form approximations to R instead (Schwind and Koditschek 2000; Bullimore et al., unpublished results; Geyer, unpublished results). For example, with absent gravity (e.g., assuming that the leg potential forces far exceed the influence of gravity during stance), the 2DoF SLIP becomes formally integrable. Indeed, our proof of the existence of "self-stable" SLIP orbits (Ghigliazza et al. 2003) applies only to this approximation. All other conclusions in that paper (and, of course, in the surrounding literature; Herr and McMahon 2000, 2001; Seyfarth et al. 2002; Seyfarth, Geyer, and Herr 2003) devolve from numerical evidence. In the case of the horizontal plane 3DoF LLS template, zeroing out the offset between the COM and hip sagittal plane affords a similarly integrable approximation with formally characterized stability properties whose applicability to the more interesting "perturbed" general case can again be ascertained only numerically (Schmitt and Holmes 2000). In the case of the sagittal plane 3DoF SLIP in gravity—the simplest implementation model for RHex, as we will explain in Altendorfer, Koditschek, and Holmes (2004)—no plausible integrable approximations have been proposed. In summary, all prior formal characterizations of 2DoF and 3DoF locomotion stability conditions have applied to approximations that ignore stance phase gravity or idealize body morphology, depending upon numerical evidence to suggest their relevance to the more general settings. Also, for RHex related models, no formal characterizations have heretofore been possible at all.

In contrast, we now present formal conditions that apply to the full parameter space of all the SLIP templates. We observe that while R cannot be written in closed form, certain physically reasonable assumptions (listed in Section 2.4.1) imply that the determinant of its Jacobian at a symmetric fixed point (to be defined in Section 2.3) of R can be so expressed. The central contributions of this paper arising from that observation are as follows.

1. A new analytical framework based on a "symmetric" factorization of the return map R, in terms of its non-hybrid components that yields the closed-form expression of the determinant at a symmetric fixed point of R (Section 3). Necessary conditions for asymptotic stability, sufficient conditions for instability, and conditions equivalent to neutral stability of the closed-loop map, R, follow.

2. Closed-form conditions on $H \circ C$ yielding rigorous statements concerning the sensory "cost" of control in both the 2DoF and 3DoF settings that cannot be established by mere numerical study, as follows.

   (a) 2DoF SLIP models: any control with fast transients ("singular" control—the Jacobian of the closed-loop return map is globally singular) requires velocity sensing and is therefore "costly" (Section 3.3.1).

   (b) 3DoF SLIP models: SLIP models that have only non-inertial (body frame) sensors available cannot implement singular control (Section 3.4).

In the companion paper (Altendorfer, Koditschek, and Holmes 2004) we explore some implications of these results for the analysis of a more detailed model inspired by RHex. The remainder of this paper is organized as follows. In Section 2 we preface this analysis by introducing the terminology and notation for hybrid systems to be used subsequently, followed by a review of how reversibility symmetries can replace the symplectic symmetry in Liouville's theorem (see, for example, Scheck 1999), which does not generally apply to hybrid systems. We then develop the consequences of these observations in Section 3 as heralded in conclusions 2(a) and 2(b). In Section 3.4 we preview a new 3DoF SLIP model inspired by RHex sagittal plane mechanics that will form the

basis of the SLIP runner studied in Altendorfer, Koditschek, and Holmes (2004). We conclude with some brief remarks in Section 4.

2. Theoretical Framework and Modeling Assumptions

In Section 2.1 we introduce the terminology of hybrid dynamical systems and provide some intuition concerning the machinery used to trim away the awkward and inessential details of our hybrid model to yield a conventional discrete dynamical control system (eq. (2)) whose closed-loop properties (eq. (1)) represent the formal object of study. Having established a notation for (hybrid) dynamical systems, Liouville's theorem, a key tool in the present study, can be stated formally in the next section, Section 2.2. Then an analogue of the local form of Liouville's theorem for discrete maps derived from hybrid systems is established in Section 2.3. In Section 2.4 we formally define the SLIP system with its hybrid components as well as its Poincaré section and discrete time return map.

2.1. Preliminary Definitions and Modeling Considerations of Hybrid Dynamical Systems

Models of legged locomotion are characterized by distinct phases, notably, stance and flight. Formally, the dynamics cannot be described by a single flow, but require a collection of continuous flows and discrete transformations governing their transitions. The resulting model is called a "hybrid" system. This section makes the notion of a hybrid system more precise by adapting the definitions in Guckenheimer and Johnson (1995) to the present setting.

Let $\mathcal{I}$ be a finite index set and $\mathcal{X}_\alpha$, $\alpha \in \mathcal{I}$ with $\dim(\mathcal{X}_\alpha) = 2N$ a collection of open Euclidean domains (charts). Assume a mechanical system whose time evolution is described by holonomically constrained autonomous conservative vector fields f_α, with configuration space variables q: $\dot{x} = f_\alpha(x)$ with $x = (q\ \dot{q})^\top \in \mathcal{X}_\alpha$. Assume that the vector fields f_α can be integrated to obtain the flow $f_\alpha^{(\cdot)}$ with $x(t) = f_\alpha^t(x_0)$. Transitions from one vector field f_α to another vector field f_β are governed by threshold functions h_α^β which specify an event at their zero-crossing. The threshold functions h_α^β depend on the initial condition $x_0 = x(t = 0) \in \mathcal{X}_\alpha$, time t; they also depend implicitly on the flow $f_\alpha^{(\cdot)}$.[1] We restrict ourselves to hybrid systems where for each chart there is only one threshold function h_α^β; hence, the upper index β will be dropped from now on. We also reset the time to zero at each chart transition. The end time of the evolution on chart $\mathcal{X}_\alpha$ is uniquely defined by $t_\alpha(x_0) = \min_{t>0}\{t : h_\alpha(x_0, t) = 0\}$. The equation $h_\alpha(x_0, t) = 0$ will be referred to as the threshold equation. Switching between charts is effected by transition mappings T_α^β with domains in $\mathcal{X}_\alpha$ and ranges in $\mathcal{X}_\beta$. The flow map F_α for the αth vector field is defined via the implicit function, t_α, $F_\alpha : x_0 \mapsto f_\alpha^{t_\alpha(x_0)}(x_0)$.[2]

In this paper, as in many settings of hybrid dynamical systems, we are interested in the attractive behavior of distinguished orbits whose appropriate projections are periodic. By "periodic" we mean that the distinguished orbit is defined on a recurring sequence of charts along which the projected flow yields a return to the same projected initial condition. An "appropriate" projection strips away variables whose values are not descriptive of the locomotion task—here, the conserved total mechanical energy along with the cyclic variable of elapsed distance. Similarly, "attractive behavior" denotes the asymptotic properties of projected orbits relative to the projection of the distinguished orbit. These slight variants of the traditional Poincaré analysis of conventional dynamical systems theory will all be introduced formally in the next section, and will be seen to yield a *stride* map

$$S = S_2 \circ S_1 \tag{4}$$

whose projection (along with those of its factors, S_α) that we will denote R (along with the corresponding factors, R_α) captures as a discrete time iterated dynamical system the locomotion relevant behavior of our hybrid dynamical system analogous to a Poincaré map.

2.2. Liouville's Theorem and Stability

Informally, Liouville's theorem states that volume in phase space of a holonomically constrained conservative dynamical system described by a single Hamiltonian flow is preserved, i.e., a set of initial conditions at $t = 0$ in phase space will be mapped to a set with identical symplectic volume for any $t \geq 0$. More formally, Liouville's theorem appears in two equivalent formulations, the local and the global form (Scheck 1999).

THEOREM 1. [Liouville's theorem (local form)] Let $f^t(x)$ be the flow of a vector field f on a chart $\mathcal{X}$ of a Hamiltonian system, i.e., $\exists H : \mathcal{X} \to \mathbb{R}$ with $\dim(\mathcal{X}) = 2N$, $N \in \mathbb{N}$ such that

$$f(x) = \begin{pmatrix} 0 & \mathbf{1}_{N\times N} \\ -\mathbf{1}_{N\times N} & 0 \end{pmatrix} D_x H(x) \quad \forall x \in \mathcal{X}. \tag{5}$$

Then, for all $x \in \mathcal{X}$ and for all times t for which the flow is defined,

$$D_x f^t(x) \in \mathrm{Sp}_{2N}; \quad \det\left(D_x f^t(x)\right) = 1 \tag{6}$$

(Sp_{2N} denotes the group of symplectic matrices of size $2N \times 2N$). The matrix of partial derivatives of the flow with respect

1. Note that this is more general than the definition in Guckenheimer and Johnson (1995), where h_α^β only depends on $f_\alpha^t(x_0)$. This added generality is required because we wish to study more general functional dependences of h_α^β on x_0 and t than the functional dependency given by $f_\alpha^t(x_0)$.

2. Note that F_α is not the usual constant-time flow map of dynamical systems theory $f_\alpha^t(x_0)$; rather, the time varies depending upon the initial data x_0.

to the initial conditions x is symplectic and its determinant is one.

The global form states that f^t maps a measurable set of initial conditions to a set of equal measure.

DEFINITION 1. [Volume preservation] A map $S : \mathcal{X} \to \mathcal{X}$ is locally volume preserving at a point $x \in \mathcal{X}$ if $|\det(D_x S(x))| = 1$. Its local volume at x is defined to be $\det(D_x S(x))$. It is volume preserving (or globally volume preserving) if $|\det(D_x S(x))| = 1 \; \forall x \in \mathcal{X}$.

This definition borrows the adjective "local" from Theorem 1 at the expense of a slight degree of imprecision in terminology, since it specifies the preservation of an infinitesimal ("local") volume at a single point.

Upon cursory inspection, it might be thought that conservative "piecewise holonomic" (Ruina 1998) systems automatically satisfy the hypotheses of Liouville's theorem. By fixing t at a particular but arbitrary time $\bar{t}$, a "degenerate" hybrid dynamical system can be defined on a single chart $\mathcal{X}_1 = \mathcal{X}$ with one vector field $f_1 = f$ and the threshold function $h_1(x_0, t) = t - \bar{t}$. The resulting stride map $S = F_1 = f^{t_1}(\cdot)$ with $t_1 = \bar{t}$ then obviously satisfies $\det(D_x S(x)) = 1 \quad \forall x \in \mathcal{X}$. However, for a threshold equation that is not purely time-dependent but also depends on $f^t(x_0)$ and x_0, the evolution time t_1 is dependent upon the initial condition, $t_1 = t_1(x_0)$, and $\det\left(D_x f^{t_1(x_0)}(x_0)\right) \neq 1$ in general. Hence, for a general hybrid dynamical system in which the threshold functions are not purely time-dependent, the determinant of the Jacobian of the stride map S (eq. (4)) cannot be expected to be of absolute value one, even if all the vector fields are Hamiltonian and all transition functions are volume preserving.

Liouville's theorem precludes the asymptotic stability of a Hamiltonian system, since an asymptotically stable equilibrium point reduces a finite phase space volume to a single point. This would require $\lim_{t\to\infty} \det(D_x f^t(x)) = 0$ for all x in the basin of attraction of the asymptotically stable equilibrium point. However, because Liouville's theorem is not guaranteed to apply, asymptotic stability of piecewise-defined holonomically constrained conservative Hamiltonian systems whose discrete time behavior can be described by an appropriate projection of a stride map S,[3] has been observed in the literature. Examples include a discrete version of the Chaplygin sleigh (Ruina 1998; Coleman and Holmes 1999) and low-dimensional models of legged locomotion in the horizontal and sagittal planes (Schmitt and Holmes 2000; Seyfarth et al. 2002; Ghigliazza et al. 2003). In all of those cases, some threshold functions are not solely time-dependent and the stride map is not volume preserving—a necessary condition for asymptotic stability. In particular, at an asymptotically stable fixed point $\bar{x}$, $|\det(D_x S(\bar{x}))| < 1$.

Having established the non-applicability of Liouville's theorem to general hybrid dynamical systems, we present criteria in the next section under which, nevertheless, the volume preservation property, $|\det(D_x S(\bar{x}))| = 1$, does indeed hold. The result could be called a point Liouville's theorem for stride map fixed points, because in distinction to the local form of Liouville's theorem, which holds for all points of symplectic phase space, our theorem only holds at fixed points, $\bar{x}$, of S.

2.3. A Point Liouville's Theorem for Hybrid Dynamical Systems

In order to prove that $|\det(D_x S(\bar{x}))| = 1$ at a fixed point of S, additional assumptions and an additional structure of the underlying vector fields f_α are needed. In particular, we require that the vector fields f_α possess a time reversal symmetry (for a survey of time reversal symmetries in dynamical systems, see Lamb and Roberts 1998; for an extensive review, see Roberts and Quispel 1992).

DEFINITION 2. [Time reversal symmetry] A vector field f on a chart $\mathcal{X}$ admits a time reversal symmetry $G : \mathcal{X} \to \mathcal{X}$ with G an involution[4] ($G \circ G = id$) if

$$D_x G \cdot f = -f \circ G \tag{7}$$

or, equivalently, if

$$G \circ f^t = f^{-t} \circ G \,. \tag{8}$$

We next introduce a further property of the stride map factors, S_α, of $S = S_2 \circ S_1$, namely that they can be written as time reversed flow maps $S_\alpha = G_\alpha \circ F_\alpha$ or $S_\alpha = F_\alpha \circ G_\alpha$. We restrict our investigation to a subset of fixed points of S, namely those that are also fixed points of the time reversed flow maps S_α. Such fixed points we will call symmetric in analogy to certain fixed points of reversible diffeomorphisms (see Definition 6 in Appendix C1). Fixed points of this kind will be shown to lie on distinguished orbits termed symmetric (Devaney 1976). Such orbits have been recognized in the prior legged locomotion literature as useful steady-state target trajectories in the control of one-legged hoppers (Raibert 1986) and also serve as steady-state target trajectories in this paper.

DEFINITION 3. **(Symmetric orbit of a time reversible vector field)** The orbit of a vector field f with time reversal symmetry G is called symmetric if it is invariant under G (Devaney 1976). This definition of symmetric orbits coincides with the notion of neutral orbits introduced in Raibert (1986) and formalized in Schwind and Koditschek (1997).

THEOREM 2. Let $\bar{x}$ be a fixed point of $S_\alpha = G_\alpha \circ F_\alpha$, where F_α is the flow map of a vector field f_α with time reversal symmetry G_α. Then $\bar{x}$ lies on a symmetric orbit of f_α.

Proof. If $\bar{x}$ is a fixed point of S_α then there exists a time $\bar{t}$ such that $G_\alpha \circ f_\alpha^{\bar{t}}(\bar{x}) = \bar{x}$. If $\bar{x}$ lies on a symmetric orbit

3. The term "piecewise holonomic system" was introduced in Ruina (1998).

4. In this paper, we restrict ourselves to involutive time reversal symmetries, although a more general definition can be found in Lamb and Roberts (1998).

then $\forall t \in [0, \bar{t}]\ \exists t' \in [0, \bar{t}] : f_\alpha^{t'}(\bar{x}) = G_\alpha \circ f_\alpha^t(\bar{x})$. Let $t' = \bar{t} - t$. Then $f_\alpha^{t'}(\bar{x}) = f_\alpha^{\bar{t}-t}(\bar{x}) \overset{(8)}{=} G_\alpha \circ f_\alpha^{t-\bar{t}} \circ G_\alpha(\bar{x}) = G_\alpha \circ f_\alpha^t \circ f_\alpha^{-\bar{t}} \circ G_\alpha(\bar{x}) \overset{(8)}{=} G_\alpha \circ f_\alpha^t \circ G_\alpha \circ f_\alpha^{\bar{t}}(\bar{x}) = G_\alpha \circ f_\alpha^t(\bar{x})$. □

Clearly, S locally preserves volume at a symmetric fixed point $\bar{x}$ if its time reversed flow maps do. On the other hand, involutions are known to be volume preserving at their fixed points.

THEOREM 3. The determinant of the Jacobian of an involution $G : \mathcal{X} \to \mathcal{X};\ \mathcal{X} \subset \mathbb{R}^N$ at a fixed point $\bar{x} \in \mathcal{X}$ of G where $\mathcal{X}$ contains a neighborhood of $\bar{x}$ is plus or minus one.

Proof.

$$\begin{aligned} G \circ G &= id \\ D_x(G \circ G)(x) &= \mathbf{1}_{N\times N} \quad \forall x \in \mathcal{X} \\ D_x G(G(x)) \cdot D_x G(x) &= \mathbf{1}_{N\times N}. \end{aligned} \tag{9}$$

Since $G(\bar{x}) = \bar{x}$, eq. (9) implies that:

$$\begin{aligned} D_x G(\bar{x}) \cdot D_x G(\bar{x}) &= \mathbf{1}_{N\times N} \\ \Rightarrow \det^2(D_x G(\bar{x})) &= 1. \end{aligned} \tag{10}$$

□

Hence a criterion for S_α being an involution is needed.

LEMMA 1. If t_α is S_α invariant, that is, $t_\alpha \circ S_\alpha = t_\alpha$ on a set $\mathcal{X}_{h_\alpha}$, then S_α is an involution on $\mathcal{X}_{h_\alpha}$.

Proof. Let $x_0 \in \mathcal{X}_{h_\alpha}$.

$$\begin{aligned} S_\alpha \circ S_\alpha(x_0) &= \\ G_\alpha \circ F_\alpha \circ G_\alpha \circ F_\alpha(x_0) &= \\ G_\alpha \circ f_\alpha^{t_\alpha(S_\alpha(x_0))} \circ G_\alpha \circ f_\alpha^{t_\alpha(x_0)}(x_0) &= \\ f_\alpha^{-t_\alpha(S_\alpha(x_0))} \circ f_\alpha^{t_\alpha(x_0)}(x_0) &= x_0\ . \end{aligned} \tag{11}$$

□

By combining Lemma 1 and Theorem 3 we can formulate the following theorem.

THEOREM 4. **(Point Liouville's theorem)** Let $\bar{x} \in \mathcal{X}_{h_\alpha}$ be a fixed point of $S_\alpha = G_\alpha \circ F_\alpha$, where F_α is the flow map of a vector field f_α with time reversal symmetry G_α. If t_α is S_α invariant on $\mathcal{X}_{h_\alpha}$ and $\mathcal{X}_{h_\alpha}$ contains a neighborhood of $\bar{x}$, then S_α is locally volume preserving at $\bar{x}$.

Proof. By Lemma 1, S_α is an involution on $\mathcal{X}_{h_\alpha}$. By Theorem 3 $|\det(D_x S_\alpha(\bar{x}))| = 1$. □

Since this theorem (in distinction to Liouville's theorem) only holds at (generally isolated) fixed points, finite volume is not preserved under S_α. However, the property of local volume preservation can be used to determine the local asymptotic behavior of discrete systems with stride maps of the form $S = S_2 \circ S_1$ at symmetric fixed points (Section 3.1.3).

For applications of Theorem 4, the condition of Lemma 1 seems to be too general to be of practical use. A more explicit condition for the S_α invariance of t_α is now given, in turn, as follows.

LEMMA 2. A necessary condition for the S_α invariance of t_α is $h_\alpha(G_\alpha \circ f_\alpha^{t_\alpha(x_0)}(x_0), t_\alpha(x_0)) = 0\ \forall x_0 \in \mathcal{X}_{h_\alpha}$.

Proof. $t_\alpha(x_0) = \min_{t>0}\{t : h_\alpha(x_0, t) = 0\}$ and $t_\alpha \circ S_\alpha(x_0) = \min_{t>0}\{t : h_\alpha(S_\alpha(x_0), t) = 0\}$. A necessary condition for t_α being S_α-invariant is $t_\alpha(x_0) \in \{t : h_\alpha(S_\alpha(x_0), t) = 0\}$, which implies $h_\alpha(S_\alpha(x_0), t_\alpha(x_0)) = 0$. Using the definition of S_α, this equation becomes

$$h_\alpha(G_\alpha \circ f_\alpha^{t_\alpha(x_0)}(x_0), t_\alpha(x_0)) = 0. \tag{12}$$

□

Assuming that $t_\alpha(x_0)$ is also the minimal solution of the threshold equation for $S_\alpha(x_0)$, it follows that the condition of Lemma 2 is also sufficient, and we conclude that t_α is invariant under S_α. Lemma 2 essentially checks that the threshold function h_α "preserves" the time reversal symmetry of f_α.

The generalization to a stride map composed of more than two time reversed flow maps S_α is straightforward. As a final observation that we will require below (in Appendix A), note that if Theorem 3 has been shown to hold for $S_\alpha = G_\alpha \circ F_\alpha$; it also holds for reverse time flow maps of the form $S_\alpha = F_\alpha \circ G_\alpha$:

LEMMA 3. If $S_\alpha = G_\alpha \circ F_\alpha$ is an involution, then $S'_\alpha = F_\alpha \circ G_\alpha$ is an involution, too.

Proof.

$$\begin{aligned} S'_\alpha \circ S'_\alpha &= F_\alpha \circ G_\alpha \circ F_\alpha \circ G_\alpha \\ &= (G_\alpha \circ \underbrace{G_\alpha) \circ F_\alpha \circ G_\alpha \circ F_\alpha}_{=id} \circ G_\alpha \\ &= G_\alpha \circ G_\alpha = id\ . \end{aligned}$$

□

2.4. SLIP Dynamics

2.4.1. Modeling Assumptions

In this section we establish the specifics of the SLIP models considered in this paper. They are listed in terms of the categories: geometry, trajectories, control, and potential forces.

Geometry. The 3DoF sagittal plane SLIP model is shown in Figure 1. It shows a rigid body of mass $\tilde{m}$ and moment of inertia $\tilde{I}$ with a massless springy leg with rest length $\tilde{\zeta}_0$ attached at a hip joint that coincides with the COM. The strength of gravity is $\tilde{g}$. The approximation of a leg with zero mass avoids impact losses at touchdown and simplifies the control. For convenience, all of the following expressions are formulated in dimensionless quantities, i.e., $t = \tilde{t}\sqrt{\frac{\tilde{g}}{\tilde{\zeta}_0}}$, $y = \frac{\tilde{y}}{\tilde{\zeta}_0}$, $\dot{y} = \frac{\dot{\tilde{y}}}{\sqrt{\tilde{\zeta}_0 \tilde{g}}}$,

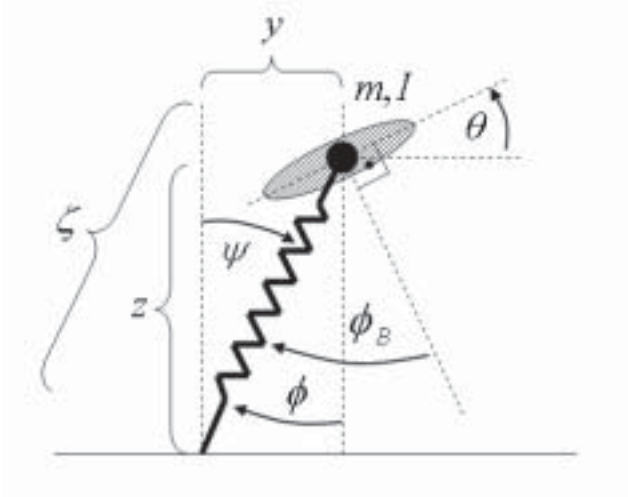

Fig. 1. Coordinate convention of SLIP with pitching dynamics. In the text, the COM coordinates are parametrized by Cartesian coordinates, i.e., $y = \zeta \sin(\psi)$ and $z = \zeta \cos(\psi)$. In flight, the leg angle ϕ is in general a function of time and of the SLIP's liftoff state: $\phi(t, x_0)$.

$z = \frac{z}{\bar{\zeta}_0}$, $\dot{z} = \frac{\dot{z}}{\sqrt{\bar{\zeta}_0 \bar{g}}}$, $\theta = \tilde{\theta}$, $\dot{\theta} = \dot{\tilde{\theta}}\sqrt{\frac{\bar{\zeta}}{\bar{g}}}$, and $I = \frac{\bar{I}}{\bar{m}\bar{\zeta}_0^2}$. Also shown are the pitch angle θ with respect to the horizontal and the parametrization of the COM in terms of Cartesian (y, z) and polar $(\zeta = \sqrt{y^2 + z^2}, \psi = \arctan(y/z))$ coordinates with the coordinate origin at the foothold. The body is assumed to remain in the sagittal plane; hence its configuration can be parametrized by $SE(2)$ coordinates[5] (y, z, θ) or (ζ, ψ, θ) of a rigid body restricted to a two-dimensional plane.

Trajectories. A full stride consists of a stance and a flight phase: in stance, we assume the foothold is fixed, the leg compressed and the body moves in the positive y direction $\dot{y} > 0$; in flight, the body describes a ballistic trajectory under the sole influence of gravity. The stance phase starts with the leg uncompressed and ends when the leg has reached its rest length $\bar{\zeta}$ again. Then the flight phase begins and ends when the massless leg (appropriately placed) touches the ground. Stability investigations in this paper are confined to trajectories that are in the vicinity of symmetric trajectories in both stance and flight, where for example the liftoff and touchdown vertical heights are equal.

Control. No continuous control is exerted during stance and flight; the corresponding vector fields do not change from stride to stride. The only control authority consists in determining the transitions between flight and stance by specifying the stance and flight time. The stance time is implicitly determined by requiring the leg to undergo a compression–decompression cycle, hence the only designable control authority consists in specifying the flight time, which can be implicitly parametrized by the free leg angle trajectory $\phi(t, x_0)$, where x_0 are the state variables taken at a certain event, e.g., leg liftoff. Because of the massless assumption, the leg can be arbitrarily placed during flight at no energetic cost.

5. $SE(2)$ denotes the Special Euclidean group in two dimensions, consisting of translations and rotations.

Potential forces.

P1 The potential energy is given by $E_p = z + V(y, z, \theta)$.

P2 The non-gravitational potential V is analytic and satisfies the symmetry relation $V(y, z, \theta) = V(-y, z, -\theta)$. This condition does not seem to severely restrict our choice of potentials, and it includes the often-used radial spring potential $V(y, z, \theta) = V_r(\zeta)$ for the 2DoF model.

P3 V factorizes as $V(y, z, \theta) = V_r(\zeta)V_p(y, z, \theta)$ with $V_r(1) = 0$. This ensures that V is zero at touchdown and liftoff. Because of the masslessness of the leg, V remains zero during flight.

After having listed SLIP's modeling assumptions, we define the stance and flight components of the hybrid SLIP system and identify time reversal symmetries present in its vector fields.

2.4.2. Definition of the Hybrid SLIP System

The SLIP system consists of two phases, stance and flight; hence, $\mathcal{I} = \{1, 2\}$ with 1 referring to stance and 2 referring to flight. In both phases, we choose the same parametrization of the configuration space: by the Cartesian coordinates of the mass center relative to the fixed toe, y, z, and the orientation of the body in the inertial frame, θ. Hence, both charts are equal, $\widehat{\mathcal{X}}_1 = \widehat{\mathcal{X}}_2 = R^2 \times \mathbb{S}^1 \times R^3 =: \widehat{\mathcal{X}}$ with phase space elements denoted by $\widehat{x} = (y, z, \theta, \dot{y}, \dot{z}, \dot{\theta})^\top$.

Stance. The stance vector field reads

$$\widehat{f}_1(\widehat{x}) = \begin{pmatrix} \dot{y} \\ \dot{z} \\ \dot{\theta} \\ -\partial_y V(y, z, \theta) \\ -1 - \partial_z V(y, z, \theta) \\ -\frac{1}{I}\partial_\theta V(y, z, \theta) \end{pmatrix}. \tag{13}$$

With **P2** this vector field is also analytic in $\widehat{x}$ and hence its flow $\widehat{f}_1^t(\widehat{x})$ is analytic in t and $\widehat{x}$. Using **P3** $\widehat{f}_1$ admits the linear time reversal symmetry

$$\widehat{G}_1 = \mathrm{diag}(-1, 1, -1, 1, -1, 1) \tag{14}$$

(the linear time reversal symmetry of eq. (13) without pitching dynamics was already recognized in Schwind and Koditschek

1997). With the "radius" function $\zeta : \widehat{x} \mapsto \sqrt{y^2 + z^2}$, the threshold function is given by

$$h_1(\widehat{x}_0, t) = \zeta(\widehat{f}_1^t(\widehat{x}_0)) - \zeta(\widehat{x}_0). \tag{15}$$

Note that ζ is $\widehat{G}_1$-invariant, i.e., $\zeta \circ \widehat{G}_1 = \zeta$.

Flight. The flight vector field reads

$$\widehat{f}_2(\widehat{x}) = \left(\dot{y}, \dot{z}, \dot{\theta}, 0, -1, 0\right)^\top \tag{16}$$

whose analytic flow is trivially computed as

$$\widehat{f}_2^t(\widehat{x}_0) = \begin{pmatrix} y_0 + \dot{y}_0 t \\ z_0 + \dot{z}_0 t - \frac{t^2}{2} \\ \theta_0 + \dot{\theta}_0 t \\ \dot{y}_0 \\ \dot{z}_0 - t \\ \dot{\theta}_0 \end{pmatrix}. \tag{17}$$

Solving eq. (7) with $\widehat{f}_2$, the diagonal linear involutive time reversing symmetry $\widehat{G}_2$ of eq. (16) is not uniquely defined and is given by

$$\widehat{G}_2^{\mp} = \mathrm{diag}(\mp 1, 1, \mp 1, \pm 1, -1, \pm 1)\ . \tag{18}$$

As will become clear later in the next section, in order to define a stride map as in eq. (4), the time reversal symmetries should match for stance and flight, hence $\widehat{G}_2^- = \widehat{G}_1 =: \widehat{G}$ is chosen.

The threshold function h_2 for a general leg placement parametrized by the angular trajectory $\phi(t, \widehat{x}_0)$ (see Figure 1) becomes zero when the toe touches the ground

$$h_2(\widehat{x}_0, t) = z(t) - \cos(\phi(t, \widehat{x}_0)) \tag{19}$$

and implicitly defines the control input $t_2(\widehat{x}_0)$. If ϕ depends on $\widehat{x}_0$, the liftoff coordinates, feedback control is employed. The design of the function ϕ constitutes the control authority in our SLIP model.

2.4.3. Discrete Time Behavior of SLIP Locomotion: Poincaré Section, Return Map, and Controlled Plant Model

Poincaré section. A SLIP stride consists of stance and flight, therefore its stride map should be written as $\widehat{S} = \widehat{F}_2 \circ \widehat{F}_1$. The end of the stance phase is characterized by the liftoff event, detected by the threshold equation h_1; the end of flight is characterized by the touchdown event, detected by the threshold equation h_2. The factorization of $\widehat{S}$ suggests a Poincaré section $\mathcal{P}$ that is the surface of the touchdown event, where the leg length is one and the COM is to the left of the foothold:

$$\mathcal{P} = \{\widehat{x} \in \widehat{\mathcal{X}} : y^2 + z^2 - 1 = 0, y < 0\}. \tag{20}$$

Return map. We would like to factor $\widehat{S}$ into time reversed flow maps $\widehat{S}_\alpha$ in order to satisfy a prerequisite of Lemma 1. This is accomplished by inserting the square of the common time reversal symmetry $\widehat{G}$:

$$\widehat{S} = \widehat{F}_2 \circ \widehat{G} \circ \widehat{G} \circ \widehat{F}_1. \tag{21}$$

However, $\widehat{S}$ does not formally constitute a return map for the Poincaré section $\mathcal{P}$, because as detailed in Section 2.4.1, trajectories of relevance to forward locomotion have a monotonically increasing fore-aft component; $y(t)$, hence, cannot be periodic. On the other hand, there is an effective projection informally built into the SLIP modeling assumption **P3**. At the beginning of stance, the y-coordinate of the coordinate origin must be reset to the new foothold in order to interpret V_r as a radial leg potential (or, more awkwardly, one could reset the definition of the potential function at each new touchdown). Both issues can be resolved by projecting out the y-entry of $\widehat{S}$. A further dimensional reduction is possible because of conservation of energy in both stance and flight phase. Formally, the total energy

$$\begin{aligned} E(\widehat{x}(t)) &= \frac{1}{2}(\dot{y}^2(t) + \dot{z}^2(t) + I\dot{\theta}^2(t)) + \\ &\quad z(t) + V(y(t), z(t), \theta(t)) \\ &=: E_0 \end{aligned}$$

can be interpreted as a constant parameter of the SLIP system and can then be used to eliminate the $\dot{y}$ variable $\dot{y}(t) = E_{x(t)}^{-1}(E_0)$,[6] with x being the projection of $\widehat{x}$ onto its "non-y, $\dot{y}$" components: $\Pi : \widehat{\mathcal{X}} \to \mathcal{X}; \quad \widehat{x} \mapsto x = (z, \theta, \dot{z}, \dot{\theta})^\top$. A return map R acting on the reduced Poincaré section $\mathcal{X} = \mathbb{R} \times \mathbb{S}^1 \times \mathbb{R}^2$ with independent coordinates x can then be written as

$$R = \Pi \circ \widehat{F}_2 \circ \widehat{G} \circ \widehat{G} \circ \widehat{F}_1 \circ \Sigma \tag{22}$$

with

$$\Sigma : \mathcal{P} \to \widehat{\mathcal{X}}; \quad x \mapsto \begin{pmatrix} -\sqrt{1 - z^2} \\ E_x^{-1}(E_0) \\ x \end{pmatrix}. \tag{23}$$

The y and $\dot{y}$ components of $\widehat{F}_2$ and $\widehat{G}$ are completely decoupled from the other components, hence the projector Π can be pulled to the right in order to define two return map factors R_α

$$R = \underbrace{F_2 \circ G}_{=:R_2} \circ \underbrace{\Pi \circ \widehat{G} \circ \widehat{F}_1 \circ \Sigma}_{=:R_1}, \tag{24}$$

where F_2 and G are the obvious restrictions of $\widehat{F}_2$ and $\widehat{G}$ to the reduced Poincaré section $\mathcal{X}$. If $\widehat{S}_\alpha$ are involutions, we want the involutive character to persist for R_α. This is obvious for $R_2 = S_2$. For R_1 it requires $\Sigma \circ \Pi = id$ on the range of $\widehat{G} \circ \widehat{F}_1 \circ \Sigma$. Let $x_1 = \widehat{G} \circ \widehat{F}_1 \circ \Sigma(x_0)$ with $x_0 \in \mathcal{P}$. y_1 is the

6. Given an equation $g(y, x) = g_0$, the corresponding implicit function will be written as $y = g_x^{-1}(g_0)$.

$\widehat{G}$-reflected y-coordinate at liftoff, hence $y_1 = -\sqrt{1 - z_1^2}$; and $\dot{y}_1 = E_{x_1}^{-1}(E_0)$. Therefore, $y_1 = \Sigma \circ \Pi(y_1)$ and R_1 is an involution if $\widehat{S}_1$ is one.

Controlled plant model. Having defined the closed-loop return map on the reduced Poincaré section, we clarify the relation of this closed-loop return map to the controlled plant model formalism introduced in Section 1.2. Since the control parameter of our SLIP model is the flight time and quantities used for feedback are the liftoff coordinates, the controlled plant model, introduced conceptually above (eq. (2)), can now be written in touchdown coordinates as

$$\begin{aligned} x(k+1) &= f_2^{t_2(k)} \circ G \circ R_1(x(k)) \\ y(k) &= C(G \circ R_1(x(k))). \end{aligned} \tag{25}$$

Using a leg angular trajectory to implement feedback control, the threshold equation implicitly defines the flight time $t_2(k)$ by

$$t_2(k) = \min_{t>0}\{t : h_2(G \circ R_1(x(k)), t) = 0\}. \tag{26}$$

Using the explicit form of h_2, eq. (19), this expression for the flight time, in turn, is a function of the control input

$$u(k) = H(y(k)) = \phi(\cdot, y(k)) \tag{27}$$

where ϕ parametrizes the leg angle trajectory in terms of the output vector $y(k)$ and the "dummy" variable t, denoted by $\cdot$.

2.4.4. Notation

The salient symbols used in this paper are next listed, with brief explanations of their meanings.

General hybrid system definitions

$\mathcal{I}$	finite index set, enumerated by α
$\widehat{\mathcal{X}}_\alpha$	chart: phase space of a dynamical system
$t, \widehat{x}$	time, chart element (dimensionless)
$\widehat{f}_\alpha$	vector field of a dynamical system on $\widehat{\mathcal{X}}_\alpha$
$\widehat{f}_\alpha^t$	flow of $\widehat{f}_\alpha$ on $\widehat{\mathcal{X}}_\alpha$
$\widehat{F}_\alpha$	flow map
T_α^β	transition function
h_α	threshold function: triggers chart transition
$t_\alpha(\widehat{x}_0)$	evolution time on chart $\widehat{\mathcal{X}}_\alpha$ starting at $\widehat{x}_0$
$\mathcal{P}$	Poincaré section (surface in $\widehat{\mathcal{X}}_\alpha$)
$\mathcal{X}_\alpha$	reduced Poincaré section
R_α	return map factor on $\mathcal{X}_\alpha$
R	return, Poincaré map

In general, an element or a map without the diacritic $\widehat{\cdot}$ denotes an element of the reduced Poincaré section $\mathcal{X}_\alpha$ or a map on $\mathcal{X}_\alpha$.

Other definitions

$\widehat{G}_\alpha$	involutive time reversal symmetry
$\widehat{\mathcal{X}}_{h_\alpha}$	set where partial stride map is an involution
$\widehat{S}_\alpha$	stride map factor on $\widehat{\mathcal{X}}_\alpha$
$\widehat{S}$	stride map
Π	projector from $\widehat{\mathcal{X}}_\alpha$ to $\mathcal{X}_\alpha$
Σ	map from $\mathcal{X}_\alpha$ to $\widehat{\mathcal{X}}_\alpha$
V	conservative SLIP potential without gravity

3. Stability and Control of SLIP Models

In this section we analyze the stability and control of SLIP models via the return map R and its factors R_α. In Section 3.1 it is first shown that the stance factor R_1 is locally volume preserving at a fixed point $\bar{x}$, independent of the specific form of the potential V as long as the conditions **P1**–**P3** are satisfied. We then derive an expression for the local volume of R_2 as a function of the leg angle trajectory ϕ. Combining these two results will give a necessary condition for stability of a SLIP model in terms of the controlled leg angle trajectory ϕ. Note that by different SLIP models we mean SLIP models that have potentials satisfying the conditions **P1**–**P3** but that differ in their leg angle trajectories ϕ.

In the remaining portions of this section, we use the preceding analysis to explore an informal relation between the "degree of stability" as manifest in the singularity of the linearized discrete return map and the "cost of feedback". The latter is judged with respect to a number of quantitative and qualitative features of known relevance in robotic implementations. These informal "cost" measures are introduced and motivated in Section 3.2 and are shown to be quantifiable using the preceding analysis. Next, in Section 3.3 we apply the results of Section 3.2 to the study of several 2DoF SLIP models (i.e., SLIP models without pitching dynamics) that have appeared in the literature, classifying them with respect to the "cost" properties previously introduced. Finally, in Section 3.4 we introduce a new 3DoF SLIP model that offers a more realistic description of the physical robot RHex operating under the influence of its open loop gait generating "clock" (Saranli, Buehler, and Koditschek 2001). We apply the analytical methods of Section 3.1, characterizing sensory "cost" and control benefit laid out in Section 3.2, and are able to give for the first time conditions on the RHex clock parameters, some necessary for gait stability, and others sufficient for gait instability.

3.1. Computation of the Local Return Map Volume

3.1.1. Stance

In this section we apply the results of Section 2.3 to show that R_1 is an involution by showing that $\widehat{S}_1$ is an involution for a SLIP model satisfying the assumptions of Section 2.4.1. We first apply Lemma 2. Given $t_1 = t_1(\widehat{x}_0)$, the threshold equation in Lemma 2 reads

$$
\begin{aligned}
&h_1(G \circ \widehat{f}_1^{t_1}(\widehat{x}_0), t_1) = \\
&\zeta(\widehat{f}_1^{t_1}(\widehat{x}_0) \circ G \circ \widehat{f}_1^{t_1}(\widehat{x}_0)) - \zeta(G \circ \widehat{f}_1^{t_1}(\widehat{x}_0)) = \\
&\zeta(G(\widehat{x}_0)) - \zeta(G \circ \widehat{f}_1^{t_1}(\widehat{x}_0)) = \\
&\zeta(\widehat{x}_0) - \zeta(\widehat{f}_1^{t_1}(\widehat{x}_0)).
\end{aligned} \tag{28}
$$

However, since this is just the negative of the original threshold equation $h_1(\widehat{x}_0, t_1) = \zeta(\widehat{f}_1^{t_1}(\widehat{x}_0)) - \zeta(\widehat{x}_0) = 0$, t_1 is also a solution of eq. (28). Assuming that $t_1(\widehat{x}_0)$ is indeed the minimal solution of the threshold equation for $S_1(\widehat{x}_0)$ for all $\widehat{x}_0 \in \widehat{\mathcal{X}}$, Lemma 2 can be applied to prove that $\widehat{S}_1$ is an involution on $\widehat{\mathcal{X}}_{h_1} = \widehat{\mathcal{X}}$. By the arguments in Section 2.4.3, R_1 is also an involution and Theorem 3 now implies that R_1 is locally volume preserving at its fixed point: $|\det(D_x R_1(\bar{x}))| = 1$.

3.1.2. Flight

We now derive a formula for the determinant of the Jacobian of the flow map F_2 given an arbitrary leg angle trajectory $\phi(t, x_0)$. This is used to compute the determinant of the Jacobian of the partial return map $R_2 = F_2 \circ G$ at a fixed point of R_2.

Note that, in contrast to R_1, $|\det(D_x R_2(\bar{x}))|$ can be computed directly for any specific leg angular trajectory ϕ using the closed-form expression of the flight phase flow eq. (17). Nevertheless, in Appendix A, Lemma 2 is applied to a particular family of leg angle trajectories in order to classify which of the resulting flight phase return maps are involutions.

The threshold function h_2 for a general leg angle trajectory ϕ is $h_2(x_0, t) = z(t) - \cos(\phi(t, x_0))$ (eq. (19)). Setting $h_2 = 0$ determines the time from leg liftoff ($t_{LO} = 0$) to leg touchdown $t_{TD} = t_2$. Because h_2 is a transcendental map, a closed-form expression for $t_2(x_0)$ cannot be found in general.

It should be pointed out that the dependence of $\phi(t, x_0)$ on the flight time t is redundant in the sense that the leg angle is irrelevant to the dynamics of the system except at the touchdown time $t_{TD}(x_0)$. Specifically, a given flight time $t_{TD}(x_0) = t_2(x_0)$ can be enforced by a purely state dependent leg angle "trajectory" $\phi(x_0) = \arccos(z(t_2(x_0)))$ or by any time-dependent trajectory $\phi'(t, x_0)$ that satisfies

$$
\phi'(t_2(x_0), x_0) = \phi(x_0) \; . \tag{29}
$$

The advantage of including time as an additional argument of ϕ will be pointed out in Section 3.3.1.

The flow map F_2 takes the state vector x_0 from its value at leg liftoff to that at touchdown: $F_2(x_0) = x(t_{TD})$. A fixed point of a symmetric flight trajectory satisfies $\bar{x} = S_2(\bar{x}) = F_2 \circ G(\bar{x})$.

The determinant of the Jacobian of $F_2(x_0) = f_2^{t_{TD}(x_0)}(x_0)$ can easily be computed from the expression for the flight phase flow (17), bearing in mind that the flight time $t_{TD}(x_0)$ also depends on the initial conditions:

$$
\begin{aligned}
&\det(D_x(F_2)(x_0)) = \\
&1 - \partial_{\dot{z}_0} t_{TD}(x_0) + \dot{z}_0 \partial_{z_0} t_{TD}(x_0) + \dot{\theta}_0 \partial_{\theta_0} t_{TD}(x_0).
\end{aligned} \tag{30}
$$

This expression exemplifies the remarks in Section 2.2, since it will reduce to one, in general, only if t_{TD} is independent of the initial conditions x_0. Hence, using implicit differentiation of eq. (19) the determinant can be written in terms of partial derivatives of $\phi(t, x_0)$

$$
\det(D_x F_2(x_0)) = 1 + \left. \frac{\Delta_2^{1\,\mathrm{num}}}{\Delta_2^{1\,\mathrm{den}}} \right|_{t=t_{TD}} \tag{31}
$$

with

$$
\begin{aligned}
\Delta_2^{1\,\mathrm{num}} &= \sin(\phi(t, x_0)) \cdot \\
&\quad \left(\partial_{\dot{z}_0}\phi(t, x_0) - \dot{z}_0 \partial_{z_0}\phi(t, x_0) - \dot{\theta}_0 \partial_{\theta_0}\phi(t, x_0)\right) \\
&\quad + t - \dot{z}_0 \\
\Delta_2^{1\,\mathrm{den}} &= \sin(\phi(t, x_0))\partial_t \phi(t, x_0) - t + \dot{z}_0 \; .
\end{aligned}
$$

Albeit t_{TD} cannot be computed in closed form in general because of the transcendental nature of h_2, we know that at a fixed point $\bar{x}$ of $F_2 \circ G$ with $\bar{x}_0 := G(\bar{x})$ the liftoff and touchdown heights are identical and hence $t_{TD} = 2\dot{\bar{z}}_0$. Therefore, $\sin(\phi(t_{TD}, \bar{x}_0)) = -\sqrt{1 - \bar{z}_0^2}$ and $\theta(t_{TD}) = -\bar{\theta}_0$. The eigenvalues of the partial return map $F_2 \circ G$ at such a fixed point are $\{1, 1, -1, -\det(D_x(F_2 \circ G(\bar{x})))\}$.

Because $G = \mathrm{diag}(1, -1, -1, 1)$, the determinants of the Jacobian of R_2 and F_2 are related as

$$
\det(D_x R_2(x)) = \det(D_x F_2(G(x))). \tag{32}
$$

2DoF SLIP model. For the 2DoF SLIP model without pitching dynamics, the $\theta, \dot{\theta}$ variables are absent and F_2, G, and R_2 are two-dimensional maps. The determinant of the flight phase flow map simplifies to

$$
\begin{aligned}
&\det(D_x F_2(x_0)) = 1 + \\
&\left. \frac{\sin(\phi(t, x_0))\left(\partial_{\dot{z}_0}\phi(t, x_0) - \dot{z}_0 \partial_{z_0}\phi(t, x_0)\right) + t - \dot{z}_0}{\sin(\phi(t, x_0))\partial_t \phi(t, x_0) - t + \dot{z}_0} \right|_{t=t_{TD}} .
\end{aligned} \tag{33}
$$

The eigenvalues of the partial return map $F_2 \circ G$ at its fixed point $\bar{x}$ are $\{1, -\det(D_x(F_2 \circ G(\bar{x})))\}$. With $G = \mathrm{diag}(1, -1)$, the determinants of the Jacobians of R_2 and F_2 are related as

$$
\det(D_x R_2(x)) = -\det(D_x F_2(G(x))) \tag{34}
$$

3.1.3. Local Volume of the Return Map at a Symmetric Fixed Point

Having derived expressions for $|\det(D_x R_1(\bar{x}))|$ and $|\det(D_x R_2(\bar{x}))|$ in the two previous sections at fixed points $\bar{x}$ of R_1 and R_2, the composition of R of those two partial return maps $R = R_2 \circ R_1$ can be used to factor the determinant

$|\det(D_x R(\bar{x}))|$ at a symmetric fixed point $\bar{x}$, i.e., a fixed point that is common to both R_1 and R_2 (see Section 2.3):

$$\begin{aligned} |\det(D_x R(\bar{x}))| &= |\det(D_x R_2(R_1(\bar{x})))| \underbrace{|\det(D_x R_1(\bar{x}))|}_{=1} \\ &= |\det(D_x R_2(\bar{x}))|. \end{aligned} \tag{35}$$

A necessary condition for local asymptotic stability of R at $\bar{x}$ is therefore $|\det(D_x R(\bar{x}))| < 1$, whereas a sufficient condition for local asymptotic instability is $|\det(D_x R(\bar{x}))| > 1$.[7] If for a certain leg angle trajectory ϕ $|\det(D_x R_2(\bar{x}))| = 1$, no conclusion about the asymptotic stability of R at $\bar{x}$ can be drawn. If, on the other hand, R_2 satisfies the point Liouville's theorem at $\bar{x}$, too, i.e., if it is an involution (see Appendix A) and if R and R_i satisfy additional conditions, then neutral stability can be concluded as detailed in Appendix C. However, the point Liouville's theorem does not allow conclusions about the preservation of a finite volume around $\bar{x}$ under R or R_i.

The factor $|\det(D_x R_2(\bar{x}))|$ is governed by the time of flight eq. (30) which in turn depends upon the functional form of the leg angle trajectory ϕ (eq. (31)). Demanding stability of R at a symmetric fixed point therefore imposes conditions on ϕ, or, using the formalism of controlled plant models, on $H \circ C$ specified in eq. (27).

3.2. Deadbeat Control and Singular Return Map Jacobians

3.2.1. Control and Sensor Modeling

For discrete systems, three different degrees of local stability can be distinguished, which are characterized by the eigenvalues of the Jacobian of the closed-loop return map at a fixed point: (i) all eigenvalues are within the unit circle; (ii) all eigenvalues are within the unit circle and some are zero ("singular control"); (iii) all eigenvalues are zero ("deadbeat control"). In general, the more singular the closed-loop return map, the quicker the transient behavior[8] but the higher the "cost" of control and the more vulnerable to modeling errors. Although we are not interested in pursuing formal optimality conditions, assessing the overall sensory cost of various control alternatives is of central concern in physical robotics applications. One reasonable approach that we adopt here is to count the number and characterize the "quality" of the sensed variables required to complete the feedback loop of the controlled plant model eq. (2). Here, "quality" refers to the frame of reference of the feedback variables, since body frame sensing is generally easier to accomplish than inertial sensing. Note that the common approach to assess different feedback laws by their energetic cost to control the system is not applicable here: according to the modeling assumptions in Section 2.4.1, the model is energy conserving and feedback control is accomplished at no energetic cost by specifying the angle trajectory $\phi(t, x_0)$ of the massless SLIP leg.

Intuitively, three different aspects of sensory cost can be readily distinguished.

S1 Detection of the event where the feedback variables are taken
(i) easy for liftoff: can be implemented in a SLIP hopper by a simple switch at the toe
(ii) difficult for flight phase apex: requires measurement of vertical velocity $\dot{z}$, either at apex ($\dot{z} = 0$), or at liftoff (detect $\dot{z}_0$ and measure time to apex $t_A = \dot{z}_0$).

S2 Enforcement of the angle trajectory ϕ: a leg angle trajectory ϕ specified with respect to an inertial frame requires inertial sensing for enforcement (i.e., feedback control), as opposed to a leg angle trajectory specified with respect to the body frame.[9]

S3 Sensing of the feedback variable x_0 by the output map C (eq. (2)):
(i) dimension of the domain (number of arguments) of C;
(ii) position versus velocity measurement: positions are in general easier to measure than velocities;
(iii) "quality": inertial versus non-inertial (body frame) quantities.

Because we exploit in this paper the factorization of R into stance and flight phase, it is natural to work in "liftoff coordinates", i.e., on the Poincaré section $\mathcal{P}$; hence, the feedback variables are naturally assumed to be taken at the "easily detected" liftoff event as noted in **S1**. We appraise in Section 3.3.1 the alternative choice of working formally in apex coordinates (not to be confused with the physically unattractive choice of taking the sensory feedback measurements at the apex event). Criteria **S2** and **S3** can be addressed by rewriting the leg angular trajectory ϕ that is defined in an inertial frame (see Figure 1) as

$$\phi(t, x_0) = \phi_C(t, C(x_0)) - \theta(t). \tag{36}$$

The second term in eq. (36) indicates that ϕ_C is specified with respect to the SLIP's body frame, as will be the case in all 3DoF SLIP models in this paper. For 2DoF SLIP models, θ is not defined and this term is absent.

It is not possible to distinguish **S3**(iii), "quality" (i.e., inertial versus non-inertial frame based) in the 2DoF setting, since by its very geometry, body frame coordinates cannot be introduced. On the other hand, the additional body pitch degree

7. Note that necessary and sufficient conditions for stability would require the knowledge of the eigenvalues of R at $\bar{x}$. However, eigenvalues of a composition of two maps do not factorize into eigenvalues of the two individual maps unless the maps commute, i.e., both are diagonalizable via the same similarity transformation.

8. This is motivated by the fact that a function from $\mathbb{R}^N$ to $\mathbb{R}^N$ whose Jacobian has rank $K < N$ everywhere maps an N-dimensional volume to a K-dimensional volume.

9. Note that this feedback control cannot be modeled straightforwardly in our simplified SLIP system because of the masslessness of the leg.

of freedom of the 3DoF SLIP model allows this distinction to be made. A leg angle trajectory that only uses sensing with respect to the body reference frame **S3**, can be modeled by the following output map C_B

$$\begin{pmatrix} \phi_{B_0} \\ \dot{\phi}_{B_0} \end{pmatrix} = \begin{pmatrix} \arccos(z_0) + \theta_0 \\ -\frac{\dot{z}_0}{\sqrt{1-z_0^2}} + \dot{\theta}_0 \end{pmatrix} = C_B(x_0) \tag{37}$$

where ϕ_{B0} is the leg liftoff angle with respect to the body normal (see Figure 1) and $\dot{\phi}_{B0}$ is the leg's angular velocity at liftoff measured in the body frame. Specifying this trajectory in the body frame yields

$$\phi(t, x_0) = \phi_{C_B}(t, \phi_{B_0}, \dot{\phi}_{B_0}) - \theta(t). \tag{38}$$

In summary, the 3DoF SLIP model allows the distinction of the "quality" of sensing required for a particular control input which in turn enables an assessment of the "cost" of control.

3.2.2. Deadbeat Control Requires Singular Return Map Jacobians

In this section, we observe that deadbeat control of a 2DoF or 3DoF SLIP model requires the Jacobian of a real-analytic return map to be globally singular, not just at the control target fixed point $\bar{x}$ but in a neighborhood $\bar{\mathcal{U}} \ni \bar{x}$ of the reduced Poincaré section $\mathcal{X}$.[10]

For the full nonlinear closed-loop plant model the return map R is deadbeat if there exists a $K \in \mathbb{N}$ such that

$$\underbrace{R \circ \cdots \circ R}_{K}(x) = \bar{x} \ \forall x \in \mathcal{X} \tag{39}$$

for a specified target $\bar{x}$. Assume K is the smallest integer for which R is deadbeat. Define

$$\begin{aligned} Q : \mathcal{X} &\rightarrow \mathcal{X} \\ x &\mapsto \underbrace{R \circ \cdots \circ R}_{K-1}(x + \bar{x}) - \bar{x} \end{aligned}$$

and $\mathcal{X}_1 := \{R(x) - \bar{x} : x \in \mathcal{X}\}$. Q is obtained by a composition of the real-analytic return map R and is therefore also real-analytic. Since R is deadbeat, $Q(x) = 0 \ \forall x \in \mathcal{X}_1$. By Łojasiewicz's structure theorem for real-analytic varieties (see Łojasiewicz 1959, chapter 15), the set $Q^{-1}(0) \cap \mathcal{U}$ with $\mathcal{U} \subset \mathcal{X}$ a neighborhood containing the origin is a finite, disjoint union of real-analytic subvarieties with dimensions less than or equal to $\dim(\mathcal{X}) - 1 = 2N - 1$. Since $\mathcal{X}_1 \subset Q^{-1}(0)$, $\mathcal{X}_1 \cap \mathcal{U}$ is also of dimension less than or equal $2N - 1$ and by continuity of R there exists a neighborhood $\bar{\mathcal{U}} \ni \bar{x}$ such that $\det(D_x R(x)) = 0 \ \forall x \in \bar{\mathcal{U}}$.

10. We are indebted to D. Viswanath for pointing out the requirement of analyticity of the return map.

3.2.3. General Solution of Leg Angle Trajectory With Singular Return Map Jacobians

As will be reviewed in Section 3.3.1, 2DoF SLIP models with globally singular return map Jacobians have featured prominently in the literature, both deadbeat and non-deadbeat. In this section we derive the general form of leg angle trajectories that render the return map Jacobian globally singular. In general, the matrix $D_x F_2$ will have full rank. If, under the influence of a particular leg angle trajectory, $\phi(t, x_0)$, the second factor of the closed-loop return map is rank deficient for all state vectors, $\det(D_x R_2(x_0)) = 0 = \det(D_x F_2(x_0))$, and if a stable fixed point exists, then, as discussed in Section 3.2.1, we would expect a "more rapid" convergence to this fixed point than if the matrix had full rank. Since eq. (31) is valid for arbitrary flight times, not just at a fixed point of R_2, a partial differential equation for globally singular leg angle trajectories $\phi(t, x_0)$ can be obtained by setting eq. (31) to zero: $\det(DF_2(x_0)) = 0$. This yields

$$\begin{aligned} &\partial_t \phi(t, x_0) + \partial_{\dot{z}_0} \phi(t, x_0) \\ &-\dot{z}_0 \partial_{z_0} \phi(t, x_0) - \dot{\theta}_0 \partial_{\theta_0} \phi(t, x_0) = 0. \end{aligned} \tag{40}$$

The general solution of this linear, homogeneous, first-order partial differential equation by the method of characteristics (Courant and Hilbert 1989) is given by

$$\phi(t, x_0) = \Phi(t - t_A, z_A, \theta_A, \dot{\theta}_A) \tag{41}$$

where Φ is an arbitrary differentiable function of its four arguments. The new variables with subscript A turn out to be apex coordinates

$$\begin{aligned} t_A &= \dot{z}_0 \\ \dot{\theta}_A &= \dot{\theta}_0 \\ z_A &= z_0 + \frac{\dot{z}_0^2}{2} \\ \theta_A &= \theta_0 + \dot{\theta}_0 \dot{z}_0 \end{aligned} \tag{42}$$

specifying the time from liftoff to apex, the pitching velocity at apex, the apex height, and the apex pitch angle. The corresponding "singularity" condition on the touchdown time t_{TD} is obtained by setting eq. (30) to zero. The general solution by the method of characteristics is again given by apex coordinates

$$t_{TD}(z_0, \dot{z}_0, \theta_0, \dot{\theta}_0) = t_A + \tau(z_A, \theta_A, \dot{\theta}_A) \tag{43}$$

with τ being an arbitrary differentiable function of its three arguments.

3.3. 2DoF SLIP Models: Sensor Requirements and Stability

In this section we focus on 2DoF SLIP models with respect to sensor requirements in their feedback loop. First, it is shown that all 2DoF SLIP models with globally singular return map

Jacobians require a measurement of the vertical velocity, either explicitly through the arguments of ϕ or implicitly. Then the dimensional reduction of the return map that follows from the globally singular return map Jacobians is illustrated with four different 2DoF SLIP models that have already appeared in the literature. A stable 2DoF SLIP model with full rank return map Jacobian is also presented to illustrate the power of our analysis in the low-dimensional setting. Since the reduced Poincaré section, $\mathcal{X}$, is only two-dimensional for the 2DoF model, the presence of complex conjugate eigenvalues of the linearized return map at a given fixed point strengthens our stability criteria to the point that the determinant magnitude condition is both necessary and sufficient for asymptotic stability. Thus, as we demonstrate, by varying one parameter, asymptotically stable, neutrally stable, and unstable behavior can be exactly assigned.

3.3.1. All Singular 2DoF SLIP Models Require Velocity Sensing

In this section several previously proposed (Raibert 1986; Geyer, Blickhan, and Seyfarth 2002; Seyfarth and Geyer 2002; Seyfarth et al. 2002; Ghigliazza et al. 2003) 2DoF SLIP control strategies are reviewed with emphasis on their globally singular return map Jacobians. The general solution for a globally singular leg angle trajectory for the 2DoF SLIP model is obtained from eq. (41) by omitting the pitch coordinates, hence $\phi(t, x_0) = \Phi(t - t_A, z_A)$. However, both control input arguments require the vertical velocity measurement $\dot{z}_0$ when expressed in liftoff coordinates eq. (42), which leaves the constant trajectory $\phi(t, x_0) = \text{const}$ as the only globally singular leg angle trajectory without explicit velocity sensing. We review four 2DoF SLIP models with globally singular leg angle trajectories, pointing out that even the leg angle trajectory $\phi(t, x_0) = \text{const}$ requires velocity sensing for its implementation as highlighted in criterion **S2**.

Constant leg touchdown angle policy. The constant leg touchdown angle policy, proposed in Altendorfer et al. (2002), Geyer, Blickhan, and Seyfarth (2002), Seyfarth et al. (2002) and Ghigliazza et al. (2003), has the simple form

$$\phi(t, x_0) = 2\pi - \beta \quad : t > t_A \tag{44}$$

where β is a constant angle for all strides. No sensing of the feedback variables **S3** is required, hence the output map C can be taken to be a constant. Since the return map Jacobian of this SLIP model is globally singular, the return map is effectively one-dimensional. In Seyfarth et al. (2002) this one-dimensional variable was taken to be the apex height, whereas in Ghigliazza et al. (2003) the angle of the touchdown velocity was chosen.[11]

A Poincaré section volume and the embedded one-dimensional return map domain is plotted in Figure 2(a), where the return map image $\mathcal{X}' := R(\mathcal{X})$ with $\mathcal{X} = [0.8, 0.99] \times [-1.5, -0.1]$ is depicted by solid points joined by a black line. The color of the points matches the color of the inverse images $R^{-1}\left(\mathcal{X}'(z_{A_i})\right)$ of these points. The color corresponds to a parametrization of the return map image in terms of the resulting apex heights z_{A_i}. Since a constant leg touchdown angle is prescribed, the touchdown height is constant and the return map image is a vertical line in $(z_0, \dot{z}_0)$-coordinates. The curved black line denotes the one-dimensional manifold of all possible fixed points for arbitrary leg angle trajectories.[12] Although ϕ is a constant and does not explicitly depend on the velocity measurement of $\dot{z}_0$, vertical velocity sensing is implicit in the derivation of the return maps in Altendorfer et al. (2002), Geyer, Blickhan, and Seyfarth (2002), Seyfarth et al. (2002) and Ghigliazza et al. (2003), because the leg angle is not held constant throughout the flight phase, but is assumed to be set to $2\pi - \beta$ in a time interval $(\dot{z}_0 - \sqrt{\dot{z}_0^2 + 2(z_0 - \sin\beta)},\ \dot{z}_0 + \sqrt{\dot{z}_0^2 + 2(z_0 - \sin\beta)})$ in which the COM is above the touchdown height $\sin\beta$. Before this time interval is reached, the leg is assumed to be at an angle where it does not interfere with the ground.

Raibert controller. The leg placement strategy proposed by Raibert (1986) for a 2DoF SLIP reads

$$\phi(t, x_0) = 2\pi - \arcsin\left(\frac{\dot{y}_0 t_s}{2} + k_{\dot{y}}(\dot{y}_0 - \dot{\bar{y}})\right) \tag{45}$$

where t_s is the duration of the stance phase, $k_{\dot{y}}$ is a feedback gain, and $\dot{\bar{y}}$ is the desired forward speed. In Raibert's physical implementations, the duration of the current stance phase was approximated by the measured duration of the previous stance phase. Here, we consider t_s a constant. In eq. (45) the average forward stance speed used in Raibert (1986) was approximated by $\dot{y}_0$. Now $\dot{y}_0$ can be expressed as $\dot{y}_0 = \sqrt{2(E - z_A)}$. Hence, eq. (45) is of the form (41) and the return map domain is a one-dimensional manifold which is depicted in Figure 2b). The output map for this leg angular trajectory reads $C(x_0) = z_A$.

11. A similar leg angular trajectory for a 3DoF SLIP model was shown in Ghigliazza et al. (2003) to yield asymptotically stable behavior for certain parameter values. Although not presented here, the return map factorization introduced in this paper can be applied to this model also to show that its stance phase is locally volume preserving at a symmetric fixed point whereas its flight phase has a globally singular return map.

12. By Theorem 2 a fixed point of the time reversed stance flow map $\widehat{S}_1$ lies on a symmetric orbit of its vector field $\widehat{f}_1$. Symmetric orbits must contain a fixed point of $\widehat{G}$ (Schwind and Koditschek 1997) and can therefore be characterized for the 2DoF SLIP model by the two-dimensional fixed point set $\text{Fix}\widehat{G} = \{\widehat{x} \in \widehat{\mathcal{X}} : y = 0, \dot{z} = 0\}$. Fixing the energy E_0 removes one dimension, hence the set of all possible fixed points of the return map factor R_1 forms a one-dimensional manifold in $\mathcal{X}$. Given that any $x = (z, \dot{z})^\top$ with $\dot{z} > 0$ lies on a symmetric orbit of the flight phase vector field f_2 on the reduced Poincaré section $\mathcal{X}$, the set of all possible fixed points of the return map R is identical to the one-dimensional manifold of possible fixed points of R_1. The fixed points of R are then given by the intersection of this line with the return map image.

Leg retraction and "optimized self-stabilization". In the leg retraction schemes proposed in Seyfarth, Geyer, and Herr (2003) and Seyfarth and Geyer (2002), the leg is set at a fixed angle α_A at the apex of the flight phase and then starts rotating towards the ground. Before reaching the apex, the leg angle can be arbitrarily placed as long as its toe does not touch the ground. In Seyfarth, Geyer, and Herr (2003), a constant angular velocity ω is used (leg retraction), i.e.,

$$\phi(t, x_0) = \alpha_A + \omega(t - t_A) \quad : t > t_A \tag{46}$$

whereas in Seyfarth and Geyer (2002) a nonlinear angular trajectory that is constant over all strides

$$\phi(t, x_0) = \alpha(t - t_A) \quad : t > t_A \tag{47}$$

is employed. In both cases, the output map is $C(x_0) = t_A$. Clearly, these two leg placement schemes are also of the form (41) and therefore the return map image is a one-dimensional manifold. These return map images are plotted in Figures 2(c) and (d), respectively. Both return maps converge to the same point; however, the second trajectory (Seyfarth and Geyer 2002) achieves convergence to a desired apex height within one stride.[13] Since the apex Poincaré section in Seyfarth and Geyer (2002) is only one-dimensional and one control parameter (the touchdown time or rather the leg touchdown angle) is available, the desired apex height can be reached within one stride. On the other hand, the touchdown Poincaré section parametrized by $(z, \dot{z})$ is two-dimensional and deadbeat control can only be achieved within at least two strides. This seems to be a contradiction, since the discrete time behavior of identical physical systems parametrized by different Poincaré sections must be conjugate, i.e., related by a coordinate transformation. Particularly, the dimension of the return maps of both parametrizations must agree. In Appendix B it is shown that if all coordinates of the dynamical flow are taken into account, the apex and touchdown return maps are indeed conjugate. However, because the open-loop system is dynamically decoupled in apex coordinates (i.e., the second variable does not influence the evolution of the first in these coordinates), restricting the feedback to depend upon the first variable yields effectively a one-dimensional closed-loop return map. This one-dimensional nature is illustrated in Figure 2d), where the one-dimensional manifold $\mathcal{X}^I := R(\mathcal{X})$ is plotted together with color-coded inverse images $R^{-1}\left(\mathcal{X}^I(z_{A_i})\right)$. As can be seen in Figure 2(d), $\mathcal{X}^I$ is aligned with one of the inverse images, hence in the first stride an arbitrary point $(z, \dot{z})$ is mapped onto $\mathcal{X}^I$, whereas in the second stride all points on this manifold are mapped to the target point.

Seyfarth and Geyer (2002) call this control scheme "optimized self-stabilization", indicating a computational or sensory advantage over regular deadbeat control. In regular deadbeat control, the leg angle ϕ would be a function of both z_0 and $\dot{z}_0$, requiring the sensing of both liftoff variables and the online computation or storage of a lookup table for a function from a two-dimensional to a one-dimensional space. In eq. (47) only the sensing of $t_A = \dot{z}_0$ and a clock is required, and α is a function from a one-dimensional to a one-dimensional space. In this context, "self-stability" seems to refer to the fact that the leg angle is a function of time (starting at apex) only and does not explicitly depend upon the liftoff variable z_0; it does not mean that no sensing (e.g., detection of the apex) is required. In the next paragraph we address the explicit parametrization of this one-dimensional return map manifold and show how it can be used to reduce the sensory requirements of control.

Sensory requirements of globally singular control. Given a globally singular 2DoF SLIP return map with leg angle trajectory $\phi(t, x_0)$, this leg angle trajectory can be rewritten as $\phi(t, x_0) = \Phi(t - t_A, z_A)$ according to the results in Section 3.2.3. The corresponding output map can be chosen to be $C(x_0) = (t_A, z_A)^\top$. This does not constitute a sensory advantage over x_0 because still one position and one velocity measurement are required. The threshold function reads

$$\begin{aligned} h_2(x_0, t) &= z(t) - \cos\left(\Phi(t - t_A, z_A)\right) \\ &= z_A - \frac{(t - t_A)^2}{2} - \cos\left(\Phi(t - t_A, z_A)\right). \end{aligned} \tag{48}$$

Setting h_2 to zero implicitly defines a function Δt_A with the substitution $t - t_A \to \Delta t_A(z_A)$. $\Delta t_A(z_A)$ encodes the direct control parameter during flight, the total flight time $t_A + \Delta t_A(z_A)$. A different angular trajectory enforcing the same total flight time for all initial conditions $z_0, \dot{z}_0$ can then be defined by the inverse Δt_A^{-1}: $\hat{\Phi}(t - t_A) := \Phi(t - t_A, \Delta t_A^{-1}(t - t_A))$ with a new output map $C(x_0) = t_A$ whose only output is the flight time measured from apex. Hence a leg angle trajectory $\phi(t, x_0)$ that initially required the sensing of $(t_A, z_A)^\top$ and time can be replaced by one that only requires sensing of the apex, i.e., $t_A = \dot{z}_0$, and time. This rewriting of the angular trajectory makes use of the invariance of the flight time with respect to certain parametrizations of ϕ (eq. (29)) and demonstrates why deadbeat control for SLIP models can be achieved with reduced feedback sensing **S3**(i).

3.3.2. A Non-Singular, Stable 2DoF SLIP Model Without Velocity Sensing

We now investigate a 2DoF SLIP model with a full rank return map Jacobian where we address both **S3**(i) and **S3**(ii) in that no velocity sensing is required for the feedback loop. For certain parameter values, this model does exhibit asymptotic stability. In the previous 2DoF examples of Section 3.3.1, once singularity has been imposed, the determinant of the return map Jacobian vanishes and the factor analysis can contribute no more information to the stabilization problem. However, as this example shows, since the return map has dimension two, if we operate in a regime where the eigenvalues are known to

13. The angular trajectory α was obtained by numerical inversion of the apex height-to-apex height return map in order to implement deadbeat control.

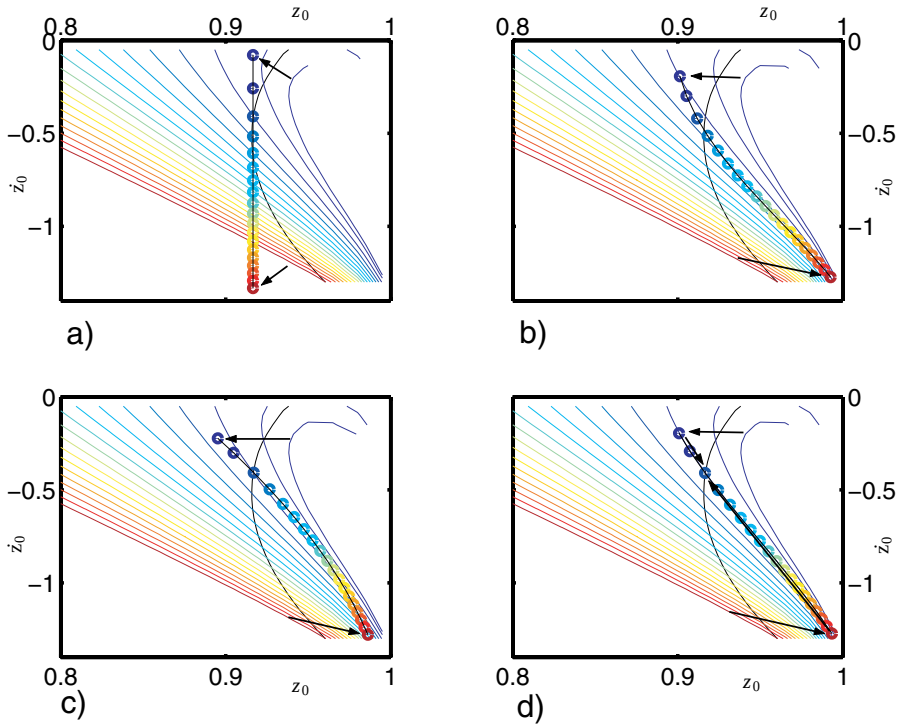

Fig. 2. One-dimensional return map domains and their inverse images for rank-deficient SLIP-controllers: (a) fixed leg angle touchdown; (b) Raibert; (c) leg retraction; (d) two-step deadbeat. All elements of a colored line in the $(z_0, \dot{z}_0)$-plane are mapped to the point with identical color. The union of all these points constitutes the return map image. The color corresponds to a parametrization of the return map image in terms of the resulting apex heights z_{A_i}. The range of apex heights considered is $z_A \in [0.92, 1.8]$. The curved black line identical in all four figures denotes the set of all possible fixed points, as explained in Footnote 12.

have non-zero imaginary components, then the properties of the determinant completely determine stability. We can then dictate the stability properties through a closed form expression and this is indeed how the present example has been adjusted.

The leg angle trajectory for this model reads

$$\phi(t, x_0) = \omega t + k \arccos(z_0) + \alpha_A \tag{49}$$

where ω, k, and α_A are constants. Note that $\dot{z}_0$ does not appear in eq. (49), hence the output map could be written as $C(x_0) = z_0$. For $k = 1$ and $\alpha_A = 0$, the leg rotates clockwise at a constant rate ω starting with the liftoff angle $\arccos(z_0)$. This can be considered a crude 2DoF SLIP version of the leg angle profile specified by RHex's open-loop controller (Saranli, Buehler, and Koditschek 2001). A more elaborate 3DoF SLIP version of RHex's open-loop controller is presented in Altendorfer, Koditschek, and Holmes 2004. Using eq. (33) the determinant of the Jacobian of R at a symmetric fixed point becomes

$$\begin{aligned} |\det(D_x R(\bar{x}))| &= |\det(D_x F_2(G(\bar{x})))| \\ &= |1 + \frac{-\dot{\bar{z}}(k-1)}{-\dot{\bar{z}} + \omega\sqrt{1-\bar{z}^2}}| \end{aligned} \tag{50}$$

$$\begin{cases} < 1 & : \quad \frac{\omega\sqrt{1-\bar{z}^2}}{\dot{\bar{z}}} < k < 1 \\ = 1 & : \quad k = 1 \\ > 1 & : \quad k > 1 \end{cases}.$$

In order to illustrate the predictive power of eq. (50), we numerically approximate the determinant $\det(D_x R(\bar{x}))$ of the full return map for fixed SLIP parameters $E_0 = \tilde{E}_0/\tilde{m}\tilde{g}\tilde{\zeta}_0 = 2.1$, $\gamma = 13$, and fixed recirculation parameters $\alpha_A = \pi$, $\omega = 14$ for different $k \in \{1/6, 0.5, 1, 2, 3.3\}$. Here, E_0 is the dimensionless total conserved energy of the system and the dimensionless spring potential is $V(\zeta) = (\gamma/2)(\zeta - 1)^2$. We then compare these values to the values of the determinant obtained by inserting the numerically determined fixed points $\bar{x} = (\bar{z}\ \dot{\bar{z}})^\top$ into eq. (50). The determinants obtained in those two different ways are plotted in Figure 3(a) and agree to a high precision ($||\det(D_x R(\bar{x}))| - |\det(D_x F_2(G(\bar{x})))|| < 10^{-7}$). In Figures 3(b)–(d) iterations of the return map in $(z_0\ \dot{z}_0)$-space are shown for $k \in \{1/6, 1, 3.3\}$ and initial conditions off the fixed point. The eigenvalues are complex conjugate pairs in all three cases; hence, the magnitude of the eigenvalues computed in eq. (50) specifies sufficient as well as necessary conditions for stability and instability in this case.

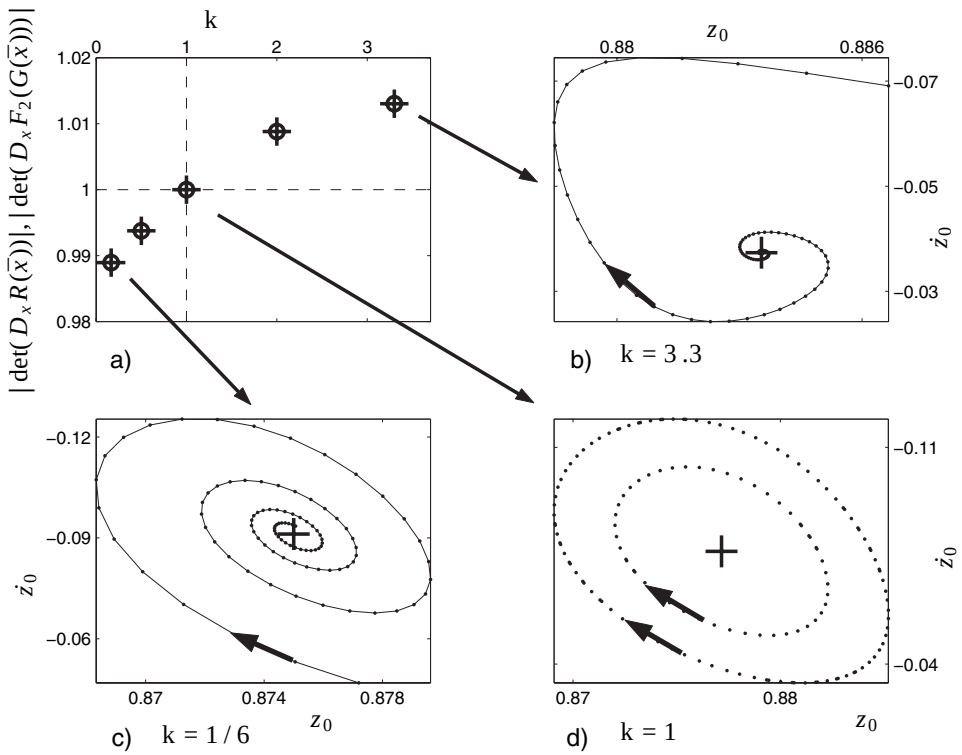

Fig. 3. (a) Comparison of the numerically computed determinant $|\det(D_x R(\bar{x}))|$ (+) of the return map Jacobian to the determinant $|\det(D_x F_2(G(\bar{x})))|$ (∘) obtained by using the numerically determined fixed points in eq. (50). (b)–(d) Trajectories around a fixed point. Because of slow convergence, only every ninth iteration in plot (b) and every fifth iteration in plot (c) are shown.

For $k = 3.3$, eq. (50) specifies an unstable fixed point, and, indeed, the plot of a numerical simulation in Figure 3(b) depicts a typical trajectory spiraling away from a small neighborhood as required. For $k = 1/6$, eq. (50) specifies asymptotic stability, and trajectories spiral towards the fixed point, as depicted in Figure 3(c). For $k = 1$, eq. (50) suggests neutral stability and numerical simulation verifies that all trajectories lie on deformed circles around the fixed point as plotted in Figure 3(d).

Figure 3(d) is reminiscent of KAM-tori of area-preserving two-dimensional mappings (see Moser 1973). However, as can be seen in Figure 4, the phase space volume is not preserved away from the fixed point $\bar{x}$ for $k = 1$. In Appendix C we invoke reversibility (Sevryuk 1986) in place of area-preservation to show that the numerically observed neutral stability for the leg recirculation scheme with $k = 1$ is expected.

3.4. 3DoF SLIP Models: Body Frame Sensing and Stability

In this final example application, we address the full 3DoF SLIP model with pitching dynamics depicted in Figure 1 that will be the basis for a RHex inspired running monoped in Altendorfer, Koditschek, and Holmes (2004). We develop two central results. First, we characterize the (unique) body frame sensor model (37) required to achieve singular control and characterize the resulting globally singular return map Jacobian. Secondly, comparing the number of available design parameters of this SLIP model to the dimension of the reduced Poincaré section, we exclude the possibility of deadbeat control.

We want to investigate the possibility of deadbeat control with a leg angle trajectory of the form (38) $\phi(t, x_0) = \phi_{C_B}(t, \phi_{B_0}, \dot{\phi}_{B_0}) - \theta(t)$, i.e., using only body frame sensor information in the feedback loop and specifying the leg angle trajectory in the body frame.

As shown in Section 3.2.2, deadbeat control requires singular return map Jacobians in a neighborhood of the fixed point and hence for deadbeat control the leg angle trajectory $\phi_{C_B}(t, \phi_{B_0}, \dot{\phi}_{B_0}) - \theta(t)$ must be of the form $\Phi(t - t_A, z_A, \theta_A, \dot{\theta}_A)$ (41). While

$$\begin{aligned} \theta(t) &= \theta_0 + \dot{\theta}_0 t \\ &= \theta_0 + \dot{\theta}_0 \dot{z}_0 + \dot{\theta}_0 (t - \dot{z}_0) \\ &= \theta_A + \dot{\theta}_A (t - t_A) \end{aligned}$$

does satisfy this functional form, $\phi_{C_B}(t, \phi_{B_0}, \dot{\phi}_{B_0})$ does not, except for $\phi_{C_B}(t, \phi_{B_0}, \dot{\phi}_{B_0}) = \text{const}$. This can be shown by rewriting the differentials in eq. (40) in terms of body coordinates:

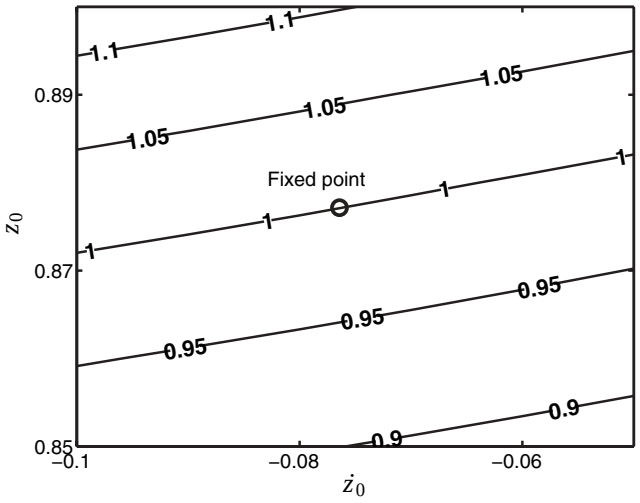

Fig. 4. Contour plot of $|\det(D_x R(\bar{x}))|$ for the leg angle trajectory (49) with $k = 1$. The fixed point $\bar{x} \approx (0.8772, -0.0764)^\top$ lies on the $|\det(D_x R(x))| = 1$ contour, whereas volume (area) is not preserved away from the fixed point.

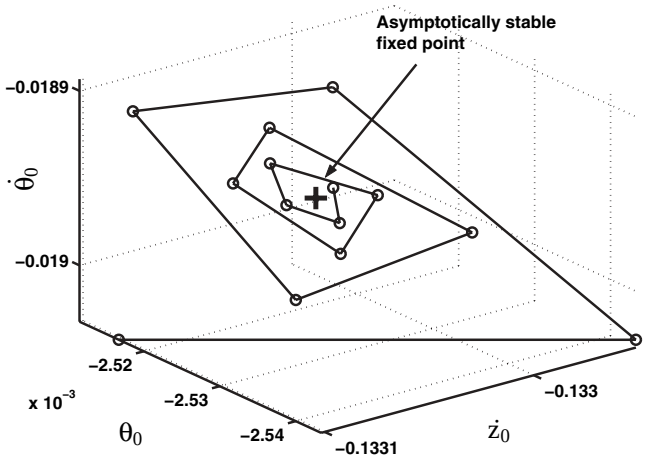

Fig. 5. A sample discrete trajectory on the three-dimensional Poincaré section parametrized by $(\dot{z}_0, \theta_0, \dot{\theta}_0)$ converging to an asymptotically stable fixed point. Because of the rank-deficient nature of the leg placement, z_0 is a function of the other Poincaré section variables $z_0 = \cos(\theta_0 + \pi/2 - \beta)$. The values of the dimensionless variables characterizing this system are $c_{\theta\theta} = 400$, $c_{\theta\psi} = -12$, $c_{\psi\psi} = 0$, $E_0 = 2.1$, $\gamma = 13.25$, $I = 0.489$, and $\beta = 1.0562$.

$$\partial_t \phi_{C_B} - \dot{\phi}_{B_0} \partial_{\phi_{B_0}} \phi_{C_B} + \frac{z_0^2 - 1 + \dot{z}_0^2 z_0}{(1 - z_0)^{3/2}} \partial_{\dot{\phi}_{B_0}} \phi_{C_B} = 0. \quad (51)$$

The coefficient

$$\frac{z_0^2 - 1 + \dot{z}_0^2 z_0}{(1 - z_0)^{3/2}}$$

cannot be written in terms of t, ϕ_{B_0}, and $\dot{\phi}_{B_0}$, hence $\partial_{\dot{\phi}_{B_0}} \phi_{C_B} = 0$. Equation (51) then implies $\partial_{\phi_{B_0}} \phi_{C_B} = 0 = \partial_t \phi_{C_B}$.

We will present numerical evidence in the form of an asymptotically stable trajectory at particular parameter values of a 3DoF SLIP model in order to show that stable behavior is possible with the leg angle trajectory

$$\phi(t, x_0) = 2\pi - \beta - \theta(t) \; . \quad (52)$$

This 3DoF SLIP model bears close resemblance to the LLS model (Schmitt and Holmes 2000) of horizontal legged locomotion, where at the end of each stance phase the new stance leg is set at a fixed angle with respect to the non-inertial body axis, thus implementing a similar leg angular trajectory.[14]

A sample discrete trajectory on the three-dimensional Poincaré section is shown in Figure 5 for a potential of the form **P3** with $V_r(\zeta) = (\gamma/2)(\zeta - 1)^2$ and $V_p(\psi, \theta) = 1 + c_{\theta\theta}\theta^2 + c_{\theta\psi}\theta\psi + c_{\psi\psi}\psi^2$. The motivation for this potential will be discussed in Altendorfer, Koditschek, and Holmes (2004). Given that the only design parameter of eq. (52) is β, a target point $(\bar{\dot{z}}, \bar{\theta}, \bar{\dot{\theta}})$ in the reduced three-dimensional Poincaré space cannot be specified a priori. Hence the possibility of deadbeat control for the 3DoF SLIP model with the body frame sensor model (37) must be discarded.

14. Note, however, that the flight duration is zero.

4. Conclusions

In this paper we use the example of the SLIP locomotion model to show how factored analysis of the return map may be a useful new tool in the stability analysis of hybrid Hamiltonian systems. Specifically, we derive a necessary condition for the asymptotic stability of SLIP for an arbitrary leg angle trajectory as well as a sufficient condition for its instability. These conditions are formulated as an exact algebraic expression despite the non-integrability of the SLIP system. Hence, leg recirculation strategies that violate the above condition can be discarded without recourse to cumbersome numerical simulations. We also use the closed-form expressions to characterize the "cost" of sensing required for the imposition of "fast" transients in a variety of 2DoF SLIP models that have appeared in the recent legged locomotion literature. Finally, we give a preview of the application of this analysis to a particular 3DoF SLIP model with pitching dynamics that will be used in the companion paper (Altendorfer, Koditschek, and Holmes 2004) as the stance phase component of a SLIP runner designed to shed light on the purely open-loop stable operation of the robot RHex.

The present paper provides a new tool to assess the stability properties of hybrid models of legged locomotion. It also paves the way for a more principled investigation of detailed, biologically-motivated leg placement strategies in the LLS model (Schmitt and Holmes 2000) which captures many aspects of insect locomotion (Schmitt et al. 2002).

Appendix A: Time Reversal Symmetry of RHex-Like Leg Angle Trajectories

In this appendix we apply the condition in Lemma 2 to a particular family of leg recirculation schemes, thus proving the involutive nature of the corresponding time reversed flow map. In particular, we prove that the solution $t_{TD}(x_0)$ of the threshold equation (19) for $S_2 = G \circ F_2$ at $x_0 \in \mathcal{X}$ for a particular leg angle trajectory also solves the threshold equation at $S_2(x_0)$. We focus on the family of leg angle trajectories

$$\phi(t, x_0) = \alpha(t) + k\,(\arccos(z_0) + \theta_0) - \theta_0 - \dot{\theta}_0 t \qquad (53)$$

where $\alpha(t)$ is an arbitrary analytic function of time. This family has the form of a RHex-like recirculation strategy used in Altendorfer et al. (2004). The threshold function $h_2(x_0, t)$ for a 3DoF SLIP model reads

$$h_2(x_0, t) = z(t) - \cos(\phi(t, x_0))\ . \qquad (54)$$

Then, using $G(x_0) = (z_0, -\theta_0, -\dot{z}_0, \dot{\theta}_0)^\top$ and

$$G \circ f_2^{t_{TD}}(x_0) = \begin{pmatrix} z_0 + \dot{z}_0 t_{TD} - \frac{t_{TD}^2}{2} \\ -\left(\theta_0 + \dot{\theta}_0 t_{TD}\right) \\ -(\dot{z}_0 - t_{TD}) \\ \dot{\theta}_0 \end{pmatrix} \qquad (55)$$

the threshold function in Lemma 2 reads

$$\begin{aligned} h_2(G \circ f_2^{t_{TD}}(x_0), t_{TD}) \quad &= \\ z_0 - \cos\Big(\alpha(t_{TD}) - \dot{\theta}_0 t_{TD} + k \arccos(z_0 + \dot{z}_0 t_{TD} - & \\ \frac{t_{TD}^2}{2}) - (\theta_0 + \dot{\theta}_0 t_{TD})(k-1)\Big) \quad &= \quad 0. \end{aligned}$$

For a solution of this equation with the leg recirculating only once during flight $\phi(t_{TD}, x_0) \in ((3/2)\pi, 2\pi)$. This must be taken into account when inverting the cosine

$$\begin{aligned} \arccos(z_0) = -\Big(&\alpha(t_{TD}) - \dot{\theta}_0 t_{TD} + \\ &k \arccos(z_0 + \dot{z}_0 t_{TD} - \frac{t_{TD}^2}{2}) \\ &-(\theta_0 + \dot{\theta}_0 t_{TD})(k-1)\Big) + 2\pi \\ \Leftrightarrow \quad \cos\left(k \arccos\left(z(t_{TD})\right)\right) - \cos\Big(&\arccos(z_0) + \alpha(t_{TD}) \\ -\dot{\theta}_0 t_{TD} - (\theta_0 + \dot{\theta}_0 t_{TD})(k-1)\Big) &= 0 \\ \overset{k=1}{\Leftrightarrow} \quad z(t_{TD}) - \cos\left(\phi(t_{TD}, x_0)\right) &= 0 \end{aligned}$$

with $\phi(t, x_0)$ as in eq. (53). For $k = 1$ this equation is equal to the original threshold equation (54) at x_0 and hence $t_{TD}(x_0)$ also solves the threshold equation for $S_2(x_0)$. Assuming that $t_{TD}(x_0)$ is also the minimal solution of the threshold equation at $S_2(x_0)$ for all $x_0 \in \mathcal{X}$, we can conclude that the time reversed flow map of the flight phase with a leg angle trajectory defined by eq. (53) with $k = 1$ is an involution on $\mathcal{X}_{h_2} = \mathcal{X}$. According to Lemma 3 this means that $F_2 \circ G = R_2$ is also an involution. Then $|\det(D_x F_2(\bar{x})| = 1$ at a fixed point $\bar{x}$.

Appendix B: Equivalence of Apex and Touchdown Poincaré Sections

In Section 3.3.1 it was noted that, in Seyfarth et al. (2002) and Seyfarth, Geyer, and Herr (2003), one-dimensional Poincaré maps characterized by the apex event during flight phase were used to illustrate the asymptotic behavior of the constant leg touchdown, leg retraction, and "optimized self-stabilization" strategies for the 2DoF SLIP model. On the other hand, straightforward counting of dimensions shows that the Poincaré section of a two-dimensional SLIP model should be two-dimensional: the dimensionless phase space $\widehat{\mathcal{X}} := \mathbb{R} \times \mathbb{R}^+ \times \mathbb{R}^2$ with elements $\widehat{x} = (y, z, \dot{y}, \dot{z})^\top$ is four-dimensional; conservation of energy $E(x) = E_0$ and the definition of the Poincaré section $\mathcal{P} := \{\widehat{x} \in \widehat{\mathcal{X}} : p(x) = 0, y < 0\}$ should reduce the dimension by two. For the Poincaré section denoting the touchdown event, $p(x) = \sqrt{y^2 + z^2} - 1$ whereas for the Poincaré section denoting the apex event, $p_A(x) = \dot{z}$. Using conservation of energy to eliminate $\dot{y}$, the reduced Poincaré sections can then be parametrized by $x = (z, \dot{z})^\top \in \mathcal{X}$ for the touchdown event and by $x_A = (y_A, z_A)^\top \in \mathcal{X}_A$ for the apex event. While for some singular leg placement strategies the reduction to a one-dimensional Poincaré section at the touchdown event is obvious, e.g., for the constant leg touchdown angle strategy illustrated in Figure 2(a), there is a priori no reason why the apex Poincaré section should only be parametrized by one variable.

In order to illustrate the equivalence of the discrete dynamical systems defined by the two different Poincaré sections, we give an explicit coordinate transformation between the coordinates of the two reduced Poincaré sections $\mathcal{X}$ and $\mathcal{X}_A$. Because of the reset of the y-coordinate at touchdown, this coordinate transformation T_A relates the touchdown variables x to the next apex variables x_A and not to the previous apex variables. It has the form

$$\begin{aligned} T_A : \mathcal{X} \quad &\to \quad \mathcal{X}_A \\ \begin{pmatrix} z \\ \dot{z} \end{pmatrix} \quad &\mapsto \quad \begin{pmatrix} y_A \\ z_A \end{pmatrix} \end{aligned}$$

where $y_A = \sqrt{1 - z_{LO}^2} + \left(\sqrt{2(E_0 - z) - \dot{z}^2}\right) \dot{z}_{LO}$ and $z_A = z_{LO} + \frac{\dot{z}_{LO}^2}{2}$ and $(z_{LO}, \dot{z}_{LO})^\top = G \circ R_1(x)$. In the notation of the controlled plant model (2), the control inputs—the apex to touchdown time $t_A = u_A$ and liftoff to touchdown time $t_{TD} = u$—are related by

$$u_A(k) = u(k) - \dot{z}_{LO}(k)\ . \qquad (56)$$

The difference between the two parametrizations arises in the structure of the controlled plant model maps A: the apex controlled plant model map A_A can be written as two separate maps A_z and A_y that are independent of $y_A(k)$ because of the y coordinate reset at touchdown:[15]

15. The formal expressions for A_z and A_y can easily be derived and are not given here.

$$\begin{aligned}(z_A(k+1), y_A(k+1))^\top &= A((z_A(k), y_A(k))^\top, u_A(k)) \\ \to z_A(k+1) &=: A_z(z_A(k), u_A(k)) \\ \to y_A(k+1) &=: A_y(z_A(k), u_A(k)).\end{aligned}$$

Hence, the only way that $y_A(k)$ can enter the apex return map R_A is through feedback: $u_A(k) = t_A(k) = t_A(z_A(k), y_A(k))$. Omitting the variable $y_A(k)$ which denotes the horizontal distance between the toe pivot and the flight phase apex, a one-dimensional return map $z_A(k+1) = A_z(z_A(k), t_A(z_A(k))) =: R_z(z_A(k))$ results. For the 3DoF SLIP model with pitching, the apex return map without $y_A(k)$ dependence reduces the dimension from four to three.

Hence, the apex Poincaré section can be a convenient parametrization since the one-dimensional character of the return map is explicit in apex coordinates if feedback is restricted to a subset of the Poincaré section coordinates not containing $y_A(k)$. The two Poincaré sections, on the other hand, are only equivalent mathematical descriptions of the same physical system and do not pose any restrictions on the leg angle trajectories. However, the touchdown Poincaré section seems to be a more natural choice for the description of physical systems, as discussed in Section 3.2.1.

Appendix C: Invariant Tori Near a Fixed Point of 2DoF SLIP Models

In this section we establish criteria for the neutral stability of fixed points of the return map R of a legged locomotion model. The closed circles in Figure 3(d) suggest the existence of one-dimensional R-invariant tori, on which R acts quasi-periodically. This is reminiscent of area-preserving mappings which can possess KAM-tori (see Moser (1973) and references therein); however, as indicated in the determinant contour plot for the stance phase alone (Figure 4), area is in general not preserved in a neighborhood of the fixed point of R, unless the leg placement policy is designed to exactly compensate for the determinant deviations of the stance phase. It is well known, on the other hand, that reversible dynamical systems can mimic the behavior of Hamiltonian systems in the sense that they can also exhibit KAM-tori (Arnol'd 1984; for a review, see Roberts and Quispel 1992). We will show how, under certain assumptions, a theorem on reversible mappings (Sevryuk 1986) can be applied to establish the existence of R-invariant tori in a neighborhood of a fixed point.

C1. Theorem on Invariant Tori Near a Fixed Point of Reversible Diffeomorphisms

Before stating the main theorem, several definitions and a lemma must be provided.

DEFINITION 4. [Involution of type (p, q)] Let $\bar{x} \in \mathbb{R}^N$ be a fixed point of the involution: $G(\bar{x}) = \bar{x}$. An involution is said to be of type (p, q) with $p + q = N$ at $\bar{x}$ if the characteristic polynomial of the Jacobian of G at $\bar{x}$ reads $(-1)^N(\lambda+1)^p(\lambda-1)^q$. This is the general form of the characteristic polynomial at the fixed point, since any involution can be written in a neighborhood of its fixed point as a partial reflection (Bochner 1945).

DEFINITION 5. [Reversible diffeomorphism] A diffeomorphism $R : \mathbb{R}^N \to \mathbb{R}^N$ is called reversible with respect to the involution G if $G \circ R \circ G = R^{-1}$.

LEMMA 4. [Composition of involutions] The composition $R = R_2 \circ R_1$ of two involutions R_1 and R_2 is reversible with respect to each of them, i.e., $R_1 \circ R \circ R_1 \circ R = id = R_2 \circ R \circ R_2 \circ R$. Likewise, a diffeomorphism R that is reversible with respect to the involution R_2 can be written as $R = R_2 \circ R_1$ where R_1 is another involution (Birkhoff 1915, section 14).

DEFINITION 6. [Symmetric fixed point of a reversible diffeomorphism] By Lemma 4 a diffeomorphism R reversible with respect to the involution R_2 can be written as $R = R_2 \circ R_1$. A fixed point $\bar{x} \in \mathbb{R}^N$ of R is called symmetric if it is also a fixed point of R_2 (Roberts and Quispel 1992).

The reduced Poincaré map for SLIP models in this paper was factorized as $R = R_2 \circ R_1$ (24). If R_1 and R_2 are involutions, then the following abridged version of theorem 2.9 in Sevryuk (1986, pp. 147–152) can be applied.

THEOREM 5. **(Invariant tori near a fixed point of a reversible diffeomorphism (Sevryuk 1986))** Let R and R_1 be diffeomorphisms $R, R_1 : \mathbb{R}^N \to \mathbb{R}^N$, analytic in a neighborhood of a common fixed point $\bar{x} \in \mathbb{R}^N$ and let R be reversible with respect to R_1. Assume that the eigenvalues $\{\lambda_i, \bar{\lambda}_i\}_{i=1,\dots,N/2}$ of the Jacobian at the fixed point $D_x R(\bar{x})$ satisfy $\lambda_i \in \mathbb{S}^1 \setminus \{-1, 1\}$ and $\{\lambda_i\}_{i=1,\dots,N/2}$ are pairwise distinct. In addition assume that R is non-degenerate, i.e., $\exists l \in \mathbb{N}$ such that $R \in \Psi_l^*$ (for a definition of Ψ_l^* see Sevryuk 1986). Then the following hold.

(a) In any neighborhood of $\bar{x} \in \mathbb{R}^N$ there exist $N/2$-dimensional tori invariant under R and R_1. The action of R on these tori is quasi-periodic, and the frequencies of this action are constant on those tori.

(b) There exist neighborhoods $\mathcal{O}_\epsilon$ of $\bar{x} \in \mathbb{R}^N$ ($\lim_{\epsilon\to 0} \operatorname{diam}(\mathcal{O}_\epsilon) = 0$, $\mathcal{O}_{\epsilon_1} \subset \mathcal{O}_{\epsilon_2}$ if $\epsilon_1 < \epsilon_2$) such that $\lim_{\epsilon\to 0} \frac{\operatorname{mes}(\mathcal{G}_\epsilon)}{\operatorname{mes}(\mathcal{O}_\epsilon)} = 1$ where $\mathcal{G}_\epsilon$ denotes the union of invariant tori in $\mathcal{O}_\epsilon$.

(c) R_1 is an involution of type $(N/2, N/2)$.

C2. Application to 2DoF SLIP Models

We now argue that this theorem can be applied to the 2DoF SLIP model with a RHex-like leg recirculation (49) with $k = 1$ as suggested by Figure 3(d). The recirculation strategy (eq. (49)) is clearly of the form (53), hence R_2 is an involution

by the result of Appendix A. In Section 3.1.1 it was shown that the partial stance return map R_1 is also an involution. Next we need to show that R_i are analytic at the fixed point $\bar{x} \approx (0.8772, -0.0764)^\top$.

Analyticity of the stance phase return map factor. In Section 2.4.2 the analyticity of the stance phase flow $\widehat{f}_1^{t(\widehat{x}_0)}$ was established. The corresponding threshold function h_1 (15) is analytic in $\widehat{x}(t)$ and $\widehat{x}_0$ if $\zeta \neq 0$. By the implicit function theorem, $t_1(\widehat{x}_0)$ will be analytic as long as

$$\frac{\mathrm{d}}{\mathrm{d}t}\left(\zeta\left(\widehat{f}_1^t(\widehat{x}_0)\right)\right)|_{t=t_1(\widehat{x}_0)} \neq 0.$$

At the fixed point $\bar{x}$, $\zeta = 1 \neq 0$ and $\frac{\mathrm{d}}{\mathrm{d}t}\left(\zeta\left(\widehat{f}_1^t(\widehat{\bar{x}})\right)\right)|_{t=t_1(\widehat{\bar{x}})} = \bar{y}\dot{\bar{y}} + \bar{z}\dot{\bar{z}} \approx 0.6829 \neq 0$. Hence, $t_1(\widehat{\bar{x}})$ is analytic at $\widehat{\bar{x}}$. Since the composition of analytic functions is analytic, $\widehat{F}_1 = \widehat{f}_1^{t_1(\widehat{\bar{x}})}(\widehat{\bar{x}})$ and $\widehat{S}_1$ are analytic at $\widehat{\bar{x}}$, and R_1 is also analytic at $\bar{x}$.

Analyticity of the flight phase return map factor. In Section 2.4.2 the flight phase flow $f_2^{t(x)}$ was seen to be analytic. We focus on the leg angle trajectory (49). The corresponding threshold function h_1 (19) is analytic in x_0 and t if $0 < z_0 < 1$. By the implicit function theorem, $t_2(x_0)$ will be analytic as long as $\frac{\mathrm{d}}{\mathrm{d}t}\left(h_2(x_0, t)\right)|_{t=t_1(x_0)} \neq 0$. At the fixed point $\bar{x}$, $0 < \bar{z} \approx 0.8772 < 1$ and $\frac{\mathrm{d}}{\mathrm{d}t}\left(h_2(G(\bar{x}), t)\right)|_{t=t_2(G(\bar{x}))} = -\dot{\bar{z}} + \sin(\omega(-2\dot{\bar{z}}) + \arccos(\bar{z}) + \pi)\omega \approx -6.6551 \neq 0$. Hence $t_2(G(\bar{x}))$ is analytic at $G(\bar{x})$. Then the composition $F_2 = f_2^{t_2(G(\bar{x}))}(G(\bar{x}))$ is analytic at $G(\bar{x})$, and S_2 and R_2 are analytic at $\bar{x}$.

If R_i are analytic, then the composition R is also analytic in $\bar{x}$ and by Lemma 4 in Appendix C1 the return map R is reversible with respect to both R_2 and R_1.

The numerically determined eigenvalue of $R : \mathbb{R}^2 \to \mathbb{R}^2$ at the fixed point $\bar{x}$ in Figure 3(d) is $\lambda_1 = -0.6956 + \mathrm{i}0.7185 \in \mathbb{S}^1 \setminus \{-1, 1\}$. The non-degeneracy condition cannot be verified rigorously due to the non-integrable nature of the return map, but is assumed to hold since degenerate diffeomorphisms are exceptional in the sense that they constitute a variety of codimension one (Sevryuk, private communication). Then the theorem predicts one-dimensional tori around the fixed point which are invariant under R and R_1 and R_2, two of which are plotted in Figure 3(d). The quasi-periodicity of the action of R is corroborated by the numerically determined trajectory of R. Theorem 5 also predicts that R_1 and R_2 are involutions of type $(1, 1)$. For the flight phase partial return map R_2 this was established in Section 3.1.2. For the stance phase partial return map, the eigenvalues of the Jacobian of R_1 at the fixed point $\bar{x}$ were numerically determined to be $\approx 1, -1$.

Acknowledgments

This work is supported in part by DARPA/ONR Grant N00014-98-1-0747 and DoE grant DE-FG02-95ER25238 (PH). Helpful discussions with D. Viswanath, R. Ghigliazza, and R. Groff are gratefully acknowledged.

References

Altendorfer, R., Moore, N., Komsuoğlu, H., Buehler, M., Brown, H.B. Jr, McMordie, D., Saranli, U., Full, R., and Koditschek, D.E. 2001. RHex: a biologically inspired hexapod runner. *Autonomous Robots* 11:207–213.

Altendorfer, R., Ghigliazza, R.M., Holmes, P., and Koditschek, D.E. 2002. Exploiting passive stability for hierarchical control. *Proceedings of the 5th International Conference on Climbing and Walking Robots (CLAWAR 2002)*, Paris, France, pp. 177–184.

Altendorfer, R., Koditschek, D.E., and Holmes, P. 2003. Towards a factored analysis of legged locomotion models. *Proceedings of the IEEE International Conference on Robotics and Automation (ICRA)*, Taipei, Taiwan, pp. 37–44.

Altendorfer, R., Koditschek, D.E., and Holmes, P. 2004. Stability analysis of a clock-driven rigid-body SLIP model for RHex. *International Journal of Robotics Research* 23(10–11):1001–1012.

Arnol'd, V.I. 1984. Reversible systems. *Nonlinear and Turbulent Processes in Physics*, R.Z. Sagdeev, editor, Harwood Academic, New York, Vol. 3, pp. 1161–1174.

Birkhoff, G.D. 1915. The restricted problem of three bodies. *Rendiconti del Circolo Matematico di Palermo* 39:265–334.

Blickhan, R. and Full, R. 1993. Similarity in multilegged locomotion: bouncing like a monopode. *Journal of Comparative Physiology A* 173:509–517.

Bochner, S. 1945. Compact groups of differentiable diffeomorphisms. *Annals of Mathematics* 46(3):372–381.

Buehler, M., Koditschek, D.E., and Kindlman, P.J. 1990. A family of robot control strategies for intermittent dynamical environments. *IEEE Control Systems Magazine* 10(2):16–22.

Coleman, M.J. and Holmes, P. 1999. Motions and stability of a piecewise holonomic system: the discrete Chaplygin sleigh. *Regular and Chaotic Dynamics* 4(2):55–77.

Courant, R. and Hilbert, D. 1989. *Methods of Mathematical Physics. Vol. 2, Partial Differential Equations*, Wiley-Interscience, New York.

Devaney, R.L. 1976. Reversible diffeomorphisms and flows. *Transactions of the American Mathematical Society* 218:89–113.

Full, R. and Koditschek, D.E. 1999. Templates and anchors: neuromechanical hypothesis of legged locomotion on land. *Journal of Experimental Biology* 83:3325–3332.

Geyer, H., Blickhan, R., and Seyfarth, A. 2002. Natural dynamics of spring-like running: emergence of self-stability. *Proceedings of the 5th International Conference on Climbing and Walking Robots (CLAWAR 2002)*, Paris, France, pp. 87–92.

Ghigliazza, R.M., Altendorfer, R., Holmes, P., and Koditschek, D.E. 2003. A simply stabilized running model. *SIAM Journal on Applied Dynamical Systems* 2(2):187–218.

Guckenheimer, J. and Johnson, S. 1995. Planar hybrid systems. *Hybrid Systems II*, Lecture Notes in Computer Science, Springer-Verlag, Berlin, pp. 202–225.

Herr, H.M. and McMahon, T.A. 2000. A trotting horse model. *International Journal of Robotics Research* 19(6):566–581.

Herr, H.M. and McMahon, T.A. 2001. A galloping horse model. *International Journal of Robotics Research* 20(1):26–37.

Holmes, P. 1990. Poincaré, celestial mechanics, dynamical systems theory and "chaos". *Physics Reports* 193(3):137–163.

Kubow, T. and Full, R. 1999. The role of the mechanical system in control: a hypothesis of self-stabilization in hexapedal runners. *Philosophical Transactions of the Royal Society of London Series B – Biological Sciences* 354(1385):849–861.

Lamb, J.S.W. and Roberts, J.A.G. 1998. Time-reversal symmetry in dynamical systems: a survey. *Physica D* 112:1–39.

Lin, P.-C., Komsuoglu, H., and Koditschek, D.E. 2003. A leg configuration sensory system for dynamical body state estimates in a hexapod robot. *Proceedings of the IEEE International Conference on Robotics and Automation (ICRA)*, Taipei, Taiwan, pp. 1391–1396.

Łojasiewicz, S. 1959. Sur le problème de la division. *Studia Mathematica* 18:87–136.

Moser, J. 1973. *Stable and Random Motions in Dynamical Systems*, Princeton University Press, Princeton, NJ.

Nakanishi, J., Fukuda, T., and Koditschek, D.E. 2000. A brachiating robot controller. *IEEE Transactions on Robotics and Automation* 16(2):109–123.

Raibert, M.H. 1986. *Legged Robots That Balance*, MIT Press, Cambridge, MA.

Rizzi, A., Whitcomb, L.L., and Koditschek, D.E. 1992. Distributed real-time control of a spatial robot juggler. *IEEE Computer* 25(5):12–24.

Roberts, J.A.G. and Quispel, G.R.W. 1992. Chaos and time-reversal symmetry. Order and chaos in reversible dynamical systems. *Physics Reports* 216:63–177.

Ruina, A. 1998. Nonholonomic stability aspects of piecewise holonomic systems. *Reports on Mathematical Physics* 42(1–2):91–100.

Saranli, U. 2000. Simsect hybrid dynamical simulation environment. Technical Report CSE-TR-437-00, University of Michigan.

Saranli, U. 2002. Dynamic Locomotion with a Hexapod Robot. PhD Thesis, University of Michigan at Ann Arbor.

Saranli, U., Buehler, M., and Koditschek, D.E. 2001. RHex: a simple and highly mobile hexapod robot. *International Journal of Robotics Research* 20(7):616–631.

Scheck, F. 1999. *Mechanics: From Newton's Laws to Deterministic Chaos*, 3rd edition, Springer-Verlag, Berlin.

Schmitt, J. and Holmes, P. 2000. Mechanical models for insect locomotion: dynamics and stability in the horizontal plane I. Theory. *Biological Cybernetics* 83:501–515.

Schmitt, J., Garcia, M., Razo, R., Holmes, P., and Full, R.J. 2002. Dynamics and stability of legged locomotion in the horizontal plane: a test case using insects. *Biological Cybernetics* 86(5):343–353.

Schwind, W.J. 1998. Spring Loaded Inverted Pendulum Running: A Plant Model. PhD Thesis, University of Michigan at Ann Arbor.

Schwind, W.J. and Koditschek, D.E. 1997. Characterization of monoped equilibrium gaits. *Proceedings of the IEEE International Conference on Robotics and Automation (ICRA)*, Albuquerque, NM, pp. 1986–1992.

Schwind, W.J. and Koditschek, D.E. 2000. Approximating the stance map of a 2DoF monoped runner. *Journal of Nonlinear Science* 10(5):533–568.

Sevryuk, M.B. 1986. *Reversible Systems*, Lecture Notes in Mathematics Vol. 1211, Springer-Verlag, Berlin.

Seyfarth, A. and Geyer, H. 2002. Natural control of spring-like running—optimized self-stabilization. *Proceedings of the 5th International Conference on Climbing and Walking Robots (CLAWAR 2002)*, Paris, France, pp. 81–85.

Seyfarth, A., Geyer, H., Günther, M., and Blickhan, R. 2002. A movement criterion for running. *Journal of Biomechanics* 35:649–655.

Seyfarth, A., Geyer, H., and Herr, H. 2003. Swing-leg retraction: a simple control model for stable running. *Journal of Experimental Biology* 206:2547–2555.

Weingarten, J.D., Lopes, G.A.D., Buehler, M., Groff, R.E., and Koditschek, D.E. 2004. Automated gait adaptation for legged robots. *Proceedings of the IEEE International Conference on Robotics and Automation (ICRA)*, New Orleans, LA, Vol. 3, pp. 2153–2158.

Westervelt, E.R., Grizzle, J.W., and Koditschek, D.E. 2003. Hybrid zero dynamics of planar biped walkers. *IEEE Transactions on Automatic Control* 48(1):42–56.

Whittaker, E.T. 1964. *A Treatise on the Analytical Dynamics of Particles and Rigid Bodies*, Cambridge University Press, Cambridge.